Science of the Total Environment 925 (2024) 171761

Contents lists available at ScienceDirect

Science of the Total Environment

journal homepage: www.elsevier.com/locate/scitotenv

Using dispersion models at microscale to assess long-term air pollution in urban hot spots: A FAIRMODE joint intercomparison exercise for a case study in Antwerp

F. Martín [a,*], S. Janssen [b], V. Rodrigues [c], J. Sousa [b], J.L. Santiago [a], E. Rivas [a], J. Stocker [d], R. Jackson [d], F. Russo [e], M.G. Villani [e], G. Tinarelli [f], D. Barbero [f], R. San José [g], J.L. Pérez-Camanyo [g], G. Sousa Santos [h], J. Bartzis [i], I. Sakellaris [i], Z. Horváth [j], L. Környei [j], B. Liszkai [j], Á. Kovács [j], X. Jurado [k], N. Reiminger [k,l], P. Thunis [m], C. Cuvelier [m]

[a] CIEMAT, Research Center for Energy, Environment and Technology, Avenida Complutense 40, 28040 Madrid, Spain
[b] VITO NV, Flemish Institute for Research and Technology, Boeretang 200, 2400 Mol, Belgium
[c] CESAM & Department of Environment and Planning, University of Aveiro, 3810-193 Aveiro, Portugal
[d] Cambridge Environmental Research Consultants (CERC), UK
[e] ENEA, Italian National Agency for New Technologies, Energy and Sustainable Economic Development, 40129 Bologna, Italy
[f] ARIANET S.r.l., via Crespi 57, 20159 Milano, Italy
[g] Computer Science School, Technical University of Madrid (UPM), Campus de Montegancedo, s/n, 28660 Madrid, Spain
[h] NILU - The Climate and Environmental Research Institute, Norway
[i] University of Western Macedonia (UOWM), Dept. of Mechanical Engineering, Sialvera & Bakola Str., 50132 Kozani, Greece
[j] SZE, Széchenyi István University, Győr, Hungary
[k] AIR&D, Strasbourg, France
[l] ICUBE Laboratory, UMR 7357, CNRS/University of Strasbourg, F-67000 Strasbourg, France
[m] European Commission, Joint Research Centre (JRC), Ispra, Italy

HIGHLIGHTS

- A modelling intercomparison for NO_2 long-term average concentrations in urban area.
- Different model approaches (CFD, Lagrangian, Gaussian, and AI) were analysed.
- The time evolution of NO_2 hourly concentrations was well estimated by all models.
- Complex models provide quite accurate one-month averaged NO_2 concentration maps.
- Monthly averages can be reliably estimated through a set of scenario CFD simulations.

GRAPHICAL ABSTRACT

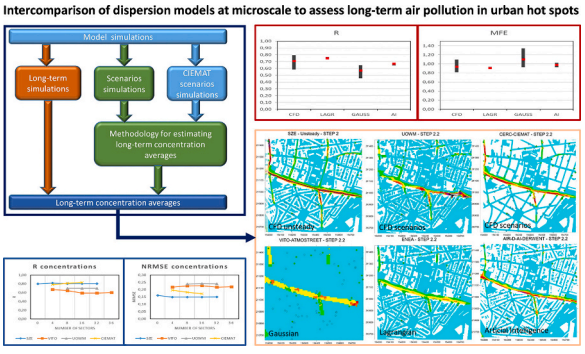

* Corresponding author.
E-mail address: fernando.martin@ciemat.es (F. Martín).

https://doi.org/10.1016/j.scitotenv.2024.171761
Received 22 December 2023; Received in revised form 8 March 2024; Accepted 14 March 2024
Available online 16 March 2024

ARTICLE INFO

Editor: Pavlos Kassomenos

Keywords:
Air pollution
Model intercomparison
Microscale modelling
Urban area
NO_2
Long-term concentration

ABSTRACT

In the framework of the Forum for Air Quality Modelling in Europe (FAIRMODE), a modelling intercomparison exercise for computing NO_2 long-term average concentrations in urban districts with a very high spatial resolution was carried out. This exercise was undertaken for a district of Antwerp (Belgium). Air quality data includes data recorded in air quality monitoring stations and 73 passive samplers deployed during one-month period in 2016. The modelling domain was 800 × 800 m^2. Nine modelling teams participated in this exercise providing results from fifteen different modelling applications based on different kinds of model approaches (CFD – Computational Fluid Dynamics-, Lagrangian, Gaussian, and Artificial Intelligence). Some approaches consisted of models running the complete one-month period on an hourly basis, but most others used a scenario approach, which relies on simulations of scenarios representative of wind conditions combined with post-processing to retrieve a one-month average of NO_2 concentrations.

The objective of this study is to evaluate what type of modelling system is better suited to get a good estimate of long-term averages in complex urban districts. This is very important for air quality assessment under the European ambient air quality directives. The time evolution of NO_2 hourly concentrations during a day of relative high pollution was rather well estimated by all models. Relative to high resolution spatial distribution of one-month NO_2 averaged concentrations, Gaussian models were not able to give detailed information, unless they include building data and street-canyon parameterizations. The models that account for complex urban geometries (i.e. CFD, Lagrangian, and AI models) appear to provide better estimates of the spatial distribution of one-month NO_2 averages concentrations in the urban canopy. Approaches based on steady CFD-RANS (Reynolds Averaged Navier Stokes) model simulations of meteorological scenarios seem to provide good results with similar quality to those obtained with an unsteady one-month period CFD-RANS simulations.

1. Introduction

Over the past few decades European cities have made significant progress in improving air quality to protect human health. Despite progress, several cities are still facing acute air pollution episodes, with various urban areas frequently exceeding European air quality standards and the guidelines established by the World Health Organization (WHO) (EEA, 2023). To reduce air pollution levels, particularly in cities where the majority of the European population lives, it is essential to define effective planning strategies to improve air quality (Rodrigues et al., 2021; Viana et al., 2020).

Numerical models have played a fundamental role in this context (Vivanco et al., 2021; Borge et al., 2018). Air quality models typically cover distinct spatial and temporal scales depending on the purpose of the application. For compliance purposes, Chemical Transport Models (CTM) have been widely used at the regional scale (Vivanco et al., 2009; Martin et al., 2014). However, their calculation grid spacing above 1 km does not resolve the high concentration gradients that occur in the vicinity of road sources, which remain the dominant source of air pollution in urban areas. Thus, modelling applications at microscale may be required when exceedances occur at local hotspots. Microscale modelling is the simulation of air quality at very high resolution (typically down to few meters) usually in urban environments. For this to be possible, factors that affect the dispersion at this level must be present explicitly or implicitly, such as urban structures (like buildings layout and roads) and how they affect wind patterns and turbulence. This type of modelling applications is increasingly used in the Ambient Air Quality Directive (AAQD) policy context (EC, 2008), driven by increased focus on urban air quality, which requires high spatial resolution to identify hotspot locations, understand the causes, determine exceedance areas and set up specific measures to mitigate or even avoid problems if considered at the urban planning stage.

At microscale, Computational Fluid Dynamics (CFD) models have been widely used to assess pollutants dispersion within street-canyons (Santiago et al., 2007; Santiago et al., 2021). CFD models accurately simulate the turbulent flow dynamics, and subsequent dispersion patterns, by solving the Navier-Stokes equations, and explicitly accounting for the complexity of the built-up environment. However, there are some limitations associated with CFD models, namely they require large computational resources to perform long-term simulations. Applications are typically available for short periods such as a single day or a few hours (Amorim et al., 2013; Sanchez et al., 2017; Rafael et al., 2018; Rivas et al., 2019). These limitations make applications associated with air quality legislation compliance challenging because there is a requirement for microscale model outputs to be aggregated to the longer temporal and spatial scales, typically a year.

Some attempts have been made to derive long-term air pollution averages in urban hotspots using CFD models. Parra et al., 2010 presented an early approach to the methodology for the derivation of long-term averages of NO_x and PM10 concentrations based on a steady-state Reynolds-Averaged Navier–Stokes equations (RANS) and standard k-ε turbulence model. CFD simulations were performed for a set of 16 different inlet wind directions over a real urban area, for two winter months, neglecting chemical reactions. Santiago et al., 2013, Santiago and Martin, 2015 and Santiago et al., 2017 applied an extension of the Parra et al., 2010 methodology using a weighted-average approach (WA CFD-RANS) to estimate the time evolution of pollutants concentration using a sequence of steady state simulations adjusting the simulated atmospheric parameters to the actual conditions at hourly frequency. NO_x maps were reconstructed using CFD simulations for different meteorological conditions covering several months, assuming non-reactive pollutants and negligible thermal effects. Sanchez et al., 2017 generated long-period average NO_x concentrations employing the same weighted-average methodology but using meteorological inflow conditions from a mesoscale model. Rivas et al., 2019 presented annual average NO_2 and NO_x concentrations over an entire city applying the WA CFD-RANS methodology. Vranckx et al., 2015 simulated the impact of trees on the dispersion of elemental carbon and PM10 in urban street canyons using the CFD OpenFOAM model. CFD simulations were performed for ten vegetation settings and a range of wind directions. The simulation results were combined using meteorological statistics and the effects of seasonal leaf loss, to determine the annual average effect of trees in street canyons.

Air quality modelling applications in urban areas have also been performed using less complex numerical methods, such as second-generation Gaussian models (Oliveira et al., 2022, Rafael et al., 2021) and Lagrangian models. Gaussian models have been routinely used for regulatory purposes in assessing the impacts on local and urban air quality of pollution sources, because they are not computationally demanding and they are easy to couple with other models like weather prediction models and chemical transport models, and in this way give fast and reliable answers in operational setups that are accessible to a wide range of users. Their conceptual basis is an idealized uniform flow with homogeneous turbulence, and they include several assumptions,

which if not followed decrease substantially the accuracy, as e.g., mean wind speed must be larger than the turbulence so that diffusion in the x direction is negligible in comparison with advection. In urban terrain, different approaches can be applied in order to adjust the effects of obstacles on wind speed vertical profiles, turbulence and dispersion parameters and/or include parameterizations of street effects on dispersion. As with other dispersion modelling approaches, they are very dependent on the reliability of the meteorological data used and the final estimate is a result of a mean flow in time and space which may not be adequate to capture concentration hotspots in a complex urban infrastructure.

Lagrangian models simulate air pollutant dispersion through virtual particles, each representing a small amount of the mass of the released substance. The average motion and diffusion of the particles are determined by the local wind, computed with a meteorological model, and the velocities derived from solving the Langevin stochastic differential equations. The equations can accurately reproduce the statistical characteristics of the turbulent flow. For example, Veratti et al. (2020) Villani et al. (2021) and Barbero et al. (2021) reconstructed the air quality in urban areas with the modelling suite PMSS, that couples a terrain-following 3D diagnostic mass-consistent model and a Lagrangian Particle Dispersion Model. In particular, the meteorological model could be run resolving the momentum equations (averaged Navier Stokes equations), initialized with the standard diagnostic solution (Carissimo et al., 2021).

Recently, the potential of using artificial neural networks (ANNs) to model the dispersion of air pollution in urban areas has been investigated with the use of a convolutional neural network (CNN) based algorithm trained on CFD results (Jurado et al., 2022). The model then demonstrated its computational efficiency on a larger scale, allowing real-time modelling at the scale of the city without compromising micro-scale phenomena, such as street canyon effects, which are generally neglected in larger scale models, or, at least, modelled through additional street canyon models (Jurado et al., 2023).

Furthermore, ambient air pollutant concentrations are a result of dispersion, chemistry and deposition processes in urban areas, short time scale NO_x chemical reactions strongly influence NO_2 concentrations at distances of a few metres from a road. Gaussian and Lagrangian models commonly account for simple NO_x chemistry while chemical reactions are rarely represented explicitly within CFD models. Some examples of including NOx chemistry in CFD models are Sanchez et al. (2016, 2017).

FAIRMODE aims to bring together air quality modelers and groups for the exchange of experiences and results from air quality modelling, thus supporting the harmonized use of modelling for air quality assessment and management between Member States, in the context of the AAQD. Within FAIRMODE, several working groups (WG) have been created to develop best practice guidance for several aspects of air quality modelling; among which the WG4 deals with microscale modelling in the context of the AAQD, i.e. air quality modelling at very high spatial resolution in urban environments, where local hotspots occur. One of the main goals of the WG4 is to test the robustness of developed methodologies to retrieve long-term averaged concentrations, and other AAQD indicators (e.g., percentiles), applying microscale models, and, overall to discuss the ability of microscale models to be used for air quality assessment and planning in the framework of the AAQD. The first activity in the WG4 was to perform an intercomparison exercise of methodologies to derive long-term pollutant concentration indicators. This allows to identify microscale modelling best practices in the context of the AAQD, by (i) assessing the importance of meteorology (e.g., understanding the differences between unsteady full year simulations and wind sector scenario approaches); (ii) specifying simulation requirements in terms of input data (e.g., microscale emission inventories, meteorological data) and observation datasets for validation, and (iii) deriving relevant information from the simulation outputs (e.g., exceedance area indicators, spatial representativeness areas of monitoring stations).

In this paper, an intercomparison of high spatial resolution air quality modelling is presented. The intercomparison is based on an exercise over an urban district of Antwerp (Belgium). The main objective of this work is to assess the suitability of distinct methodologies for computing long-term average air pollutant concentration maps in urban hot spots. The paper is organized as follows: in Section 2, the numerical modelling approaches are described in detail, followed by a description of the application specificities of the selected area, of the input data, and of the selected statistical indicators. Section 3 presents the results of the comparison of the modelling estimates with observations. In Section 4, those results and their implications are discussed. Finally, conclusions are given in Section 5.

2. Methodology

2.1. Description of the input data and exercise settings

The model intercomparison is set up for an urban district of the city of Antwerp (800 × 800 m^2), Belgium; this district is an urban built-up area, typical of North-West European cities, consisting of a mix of street canyons and open areas. The majority of the buildings are 2 or 3 floor residential houses with small private gardens in the backyard. Commercial and residential buildings of varying heights are located along the main road (Plantin en Moretuslei) crossing the area in the East-West direction. The density of buildings in the domain was 40.7 %. The height of the buildings is mostly <16 m. However, there are some tall buildings (>30 m high even reaching >40 m high in a few cases) in different parts of the domain, but more concentrated in the main avenue. The layout of the study area is depicted in Fig. 1.

Two automated fix monitoring AQ stations operated by the Flemish Environment Agency (VMM) are positioned along the main road (Fig. 1). The traffic station (42R802) is located 7 m away from the kerb, while the urban background station (42R801) is located at a distance of 30 m from the first traffic lane. NO_2 data is collected on an hourly basis at both stations alongside other air pollutants including PM10, PM2.5, O_3 and BC. Hourly NO_2 concentrations representing the transport of pollutants into the study area are provided by the RIO model (Janssen et al., 2008). The RIO model is a detrended Ordinary Kriging interpolation model used to derive regional background concentrations based on measurements recorded by the automated monitoring network (Janssen et al., 2008). RIO NO_2 concentrations are derived at an hourly frequency and are deemed to be representative of the urban background (or rooftop) concentrations.

The official monitoring network data is complemented by the results of a passive sampling campaign, organized by the University of Antwerp, in the context of the citizen science project CurieuzeNeuzen (https://ringland.be/academie/curieuzeneuzen/overzicht/). In total, about 2000 passive samplers were distributed among Antwerp's citizens to collect data during the period 2016-04-30 to 2016-05-28. At each location, NO_2 concentration values recorded by 73 samplers within the study area, averaged over this period, are available for model evaluation. The sampling data has been collected, validated and quality controlled according to the procedures described in De Craemer et al. (2020) and Hooyberghs et al. (2022).

Meteorological data recorded at the VMM measurement station M802 at Antwerp-Luchtbal (Location: 51.261, 4.425) was used by some models; this station is classified as an urban background location. Meteorological parameters recorded include wind speed components (m/s, measured at 30 m), temperature (K, measured at 3 m), relative humidity (%, measured at 3 m) and total radiation (W/m^2, measured at 3 m), all available at hourly frequency.

Traffic emissions are available for a selection of major and secondary roads (see Fig. 2) from the official Flemish FASTRACE traffic emission model (version 2.1), based on COPERT 5 emission factors. Emission factors are combined with modelled traffic flows and recordings of the

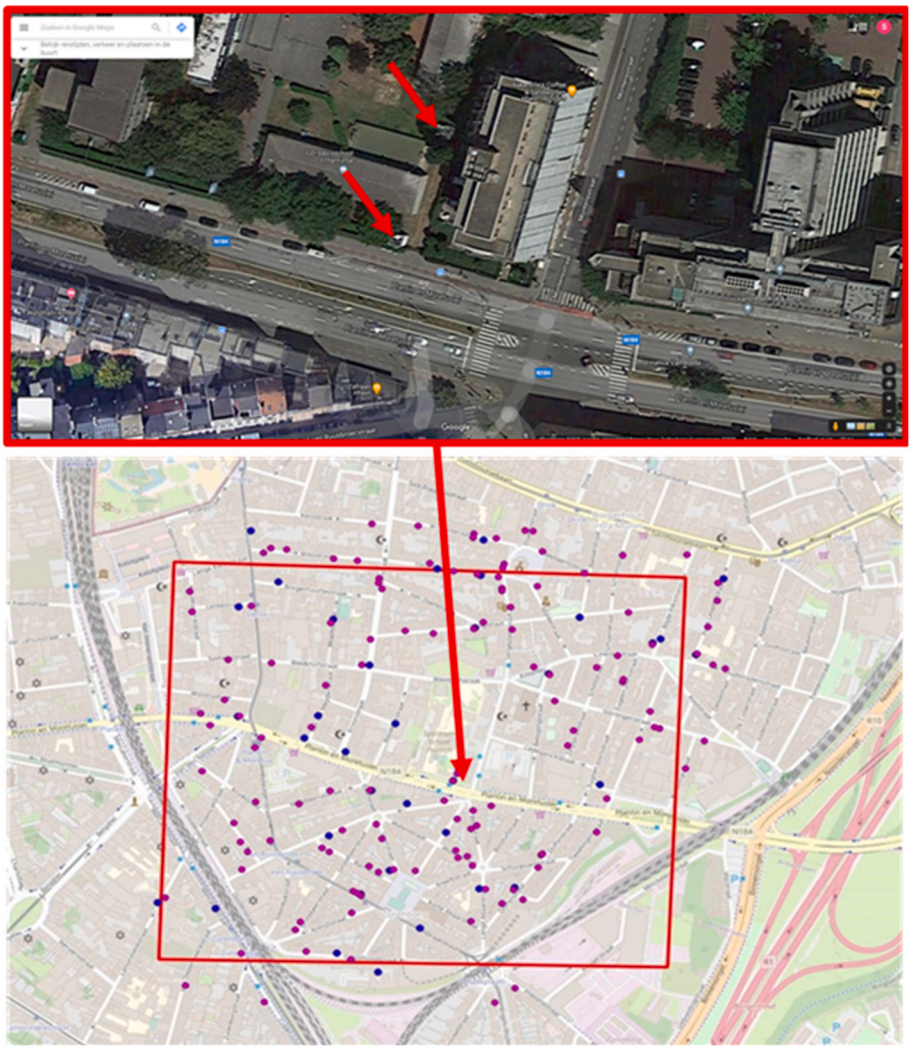

Fig. 1. Modelling domain (aprox 800 × 800 m^2) in the city of Antwerp, Belgium (red rectangle). Pink dots represent the locations of the passive samplers in the study area (blue dots are related to a second campaign not used in this study). Red arrows indicate the location of the official monitoring stations 42R801 and 42R802 along the major road Plantin en Moretuslei.

fleet composition for the year 2016 (Department for Mobility). For each line segment, NOx and NO2 emission are available in g/m/y complemented by information about the road type: U (urban), R (rural) or H (highway), the free-flow speed (in m/s), the number of light (cars + LDV) and heavy vehicles (HDV + bus) per year. Finally, monthly and daily time profiles (Department of Mobility) are used to derive hourly emissions.

All the mentioned datasets (measurements, meteorology, emissions, and background concentrations) are available on an hourly basis for the entire year of 2016. Only for the passive sampling campaign data are limited to a monthly average for the month of May. Background concentrations as well as the emission database was common to all partners.

2.2. Description of the modelling applications

Various models and model applications were used to compute the long-term averaged pollutant concentrations. In this study, model stands for the software, which was used, while model application indicates the method applied to compute the long-term averaged pollutant concentrations. While some methods were based on simulating a set of scenarios, most commonly employing the CFD RANS steady state approach, others were based on performing CFD unsteady state simulations, performing a full month simulation with non-CFD approaches and applying a convolutional neural network. Detailed information is provided in Tables 1, 2 and 3. All the CFD simulations were performed neglecting chemical reactions by assuming a passive scalar pollutant and only neutral atmospheric stability conditions were imposed.

The main limitations of the CFD approaches are associated with neglecting thermal effects and considering non-reactive pollutants. Furthermore, for steady state simulations, concentrations at a specific hour are assumed to only depend on the emissions within the computational domain, and on meteorological conditions and background values for that specific hour. The assumption of Reynolds independence entails a linear relation between concentrations and wind speed which has been verified both numerically and in wind tunnels for momentum free sources (Schatzmann and Leitl, 2011).

For the scenario-based approaches, the number of scenarios varied from 16 wind sectors (four of the modelling applications) to a maximum of 36 wind sectors using VITO's OpenFOAM application. However, when investigating what number of scenarios are better, results for other different number of scenarios starting at four scenarios has been analysed. Distinct procedures were implemented for retrieving annual or monthly average concentrations. These include the reconstruction of hourly concentration maps by assigning a representative scenario to each hour in the time series and applying a linear correction for the wind speed and the emissions or by applying weighted averages of the

Fig. 2. Line segments with modelled traffic flow used in the FASTRACE model to derive traffic emissions. The red square represents the modelling domain.

scenarios based on probability density functions.

In contrast to the scenario-based approaches, a number of models were able to compute directly hour by hour time series for either the full month or episodes. These are models such as Gaussian plume models with and without street canyon parameterizations, a Lagrangian model, an Eulerian dispersion model with imbedded Gaussian model, a CFD-LES (CFD-Large Eddy Simulation) and a CFD-RANS unsteady state. These simulations were performed considering the distinct modelling approaches, distinct methods to include urban morphology, distinct sizes of computational domain, grid types, resolution and total number of cells used to characterize those simulations, applying a wide range of approaches to account for chemistry reactions, atmospheric stabilities, and meteorology data. On the other hand, the different methods were more aligned concerning emissions.

Each model had its own model domain but all of them included a common 800 × 800 m^2 domain for the model intercomparison (see Fig. 1).

Concerning the computational cost of running this model applications, (model simulations plus, in some cases, postprocessing for retrieving long-term pollutant concentration), it depends on the complexity of the model and the computer power. Some models, like CFD models, require high-performance computers, but others can operate on personal computers. The most expensive option is the unsteady full period CFD simulation. This type of simulations is not usually affordable in most cases. In this study, the SZE group used a very powerful supercomputer, which is not easily available for most, spending several weeks to run a full-year unsteady CFD simulation. This makes the use of other approaches or models necessary. In contrast, other approaches such as scenario-based CFD simulations need several hours or a few days to simulate all the scenarios and less than an hour to compute the long-term averages. Other models such as Gaussian, Lagrangian, and AI models also need a few hours or even less than 1 h in the case of the simplest models.

2.3. Description of the intercomparison exercise

The modelling applications were used to calculate the monthly averaged NO_2 within the 800 × 800 m^2 domain (Fig. 1), where two AQ stations are sited. The monthly period goes from April 30th to May 28th, 2016, which corresponds to the duration of the passive sampler campaign described in Section 2.1.

During the campaign period (April 30th-May 28th, 2016), the weather was mostly clear skies or with few clouds, with 8 rainy days (total precipitation was 54 mm). The average temperature was 15 °C ranging from 2.7 to 26.9 °C. Wind speed ranged from 0.3 to 7.8 m/s and there were 3 dominant wind directions: NNW (12.5 % of the cases), E (10.04 %), and SW (10.02 %). The average NO_2 concentrations were 35 and 36 μg/m^3 in the background and traffic air quality stations, respectively. The maxima hourly concentrations were 173 and 178 μg/m^3, respectively, which happened on May 6th.

Previously the performance in estimating the hourly time series NO_2 concentrations for the day of highest pollution (May 6th, 2016) at the two air quality monitoring locations have been analysed (see Supplementary material). The computed NO_2 average concentration for the campaign period were compared with the measured data from the 73 samplers deployed in the computational domain (see Fig. 1). Additionally, the computed 2D concentration maps were intercompared.

Both graphical and statistical analysis were performed. In terms of the graphical analysis, scatter plots and 2D maps were employed.

Statistical analysis was carried out using the following statistical metrics:

1. Pearson correlation coefficient (*R*):

$$R = \frac{1}{N-1}\sum_{i=1}^{N}\frac{(M_i-\overline{M})(O_i-\overline{O})}{\sigma_M\sigma_O}$$

2. Mean Fractional Bias (*MFB*):

Table 1
Description of the models (and model setup) used for directly estimating the monthly average concentrations with full period simulations on an hourly basis.

Institution	VITO	CERC	ENEA	NILU	UPM	SZE
Model	ATMOStreet	ADMS	PMSS	EPISODE	PALM4U	OpenFOAM
Description	Gaussian plume (IFDM) with street canyon parameterization (OSPM)	Quasi-Gaussian	Mass consistent diagnostic reconstruction + conservation of momentum for meteorology & obstacle aware Lagrangian dispersion	3D grid Eulerian dispersion model with imbedded Gaussian dispersion model	CFD-LES	CFD Unsteady RANS with k-eps turbulence modelling
Urban morphology	Building footprints and heights	Buildings data processed to generate road by road street canyon, and gridded building, parameters. Parameters used to model dispersion in street canyons and within the urban canopy.	Data provided by VITO. Buildings simplified and grouped in blocks.	None.	Data provided by VITO. 3D buildings as cubes (5x5x5 m)	Data provided by VITO.
Computational domain	Full Antwerp city	Model input horizontal domain: 7822 m × 7750 m. Vertically, model extends to above the boundary layer.	Buildings within an 800 m × 800 m region centered in the AQ station. No distance is needed from buildings to lateral boundaries; height of domain = 500 m; Hmax = height of tallest building	Larger domain defining all the road net available. The 3D grid had the resolution of 1 kmx1kmx20m. Then in the smaller 800mx800m domain we set points at the passive samplers' locations and regularly in 20mx20m and at a 2 m height.	3D grid: 200 (x) x 200 (y) x 70 (z) grid cells. 5 m spatial resolution.	2.6 km × 2.6 km with buildings in AOI. 8.6kmx8.6 km total simulation domain. Height of domain = 400 m
Grid type	Receptor points	Irregular, source oriented. Higher receptor network where concentrations gradients are highest.	Regular horizontal grid, terrain following vertical grid with 17 levels	Regular	Regular	Octree mesh.
Grid resolution	10 m	From 0.3 m to 25 m	3 m horizontal resolution	1kmx1km and 20mx20m	5 m 200 × 200 grid cells	2 m on ground level, up to 32 m in the outside of the area of interest
Total number of cells				81 and 1600		3.3 million
Emissions data	Computed using the FASTRACE model, and applying time profiles	Traffic emission data, together with the temporal profiles provided by VITO		Traffic emission data, together with the temporal profiles provided by VITO, except for hourly profiles	Traffic emission data, together with the temporal profiles provided by VITO	
Chemistry	Simple chemistry	NO_x photolytic chemistry module, which accounts for fast, near-road oxidation of NO by O_3 to form NO_2	No chemistry, passive pollutant. NOx/NO2 transformation as post-processing based on NOx/NO2 ratio of RIO model	Calculations of NO2 are based on using photochemical equilibrium between the three fast-cycle reactive compounds NO, NO2 and O3.	Photo-stationary. Chemistry mechanism	No chemistry yet. Passive scalar pollutant.
Atmospheric stability	Stable, neutral and unstable	Full range, characterized by ratio of boundary layer height to Monin-Obukhov length	Depending on meteorological conditions and parameterized through Surface Layer scaling variables	Pasquill-Guifford stability class.	Stability dependent simulation	Neutral conditions
Meteorological boundary conditions	Data from the meteorological station: Antwerpen-Luchtbal.	Measured meteorological data in Antwerp (VITO data) adjusted to account for the change in roughness at the meteorological measurement station compared to the dispersion site.	Data from the meteorological station: Antwerpen-Luchtbal.	WRF was configured in a system with 3 one-way nested domains until the 1 kmx1km resolution for the larger domain.	From WRF/Chem simulation 1 km spatial resolution Off-line nesting, BCs frequency 10 min. Wind components (u, v, w). Potential temperature and humidity. Soil temperature and moisture.	Logarithmic boundary wind profile based on data from the meteorological station: Antwerpen-Luchtbal.
Meteorology within the domain				We used the data from the meteorological model WRF in the 1		Diffusion coefficients depend on PBL height and

(*continued on next page*)

Table 1 (*continued*)

Institution	VITO	CERC	ENEA	NILU	UPM	SZE
				kmx1km horizontal resolution.		turbulence diffusion coefficient.
Pollution boundary conditions/ background concentrations	Background concentrations provided by RIO model.			For NO2 and NO we used RIO background and for O3 we used observations available.	From WRF/Chem simulation 1 km spatial resolution Off-line nesting, BCs frequency 10 min.	Background concentrations provided by RIO model.
Assumptions and/ or limitations	Gaussian plume parameterization. No account for explicitly 3D effects. Street canyon parameterization (OSPM model)	Street canyon flow and dispersion assumes uniform properties along the length of each modelled road with well-established flow patterns (no specific modelling of individual buildings or junctions); thermal effects on in-canyon flow (e.g., differential solar heating) neglected; concentration at a selected hour only depends on the emissions within the modelling domain and meteorological conditions at that hour.		Gaussian plume model for the dispersion from the roads. No buildings accounted. Meteorology data from a model with coarse resolution, which means that for the 800mx800m we worked with two data points. Simplified meteorology in the 3D eulerian grid.		Diffusion coefficients equal in each direction.
References	Hooyberghs et al. (2022)	Zhong et al. (2021), Hood et al. (2021), Biggart et al. (2020), Owen et al. (2000), Carruthers et al. (1994)	Oldrini et al. (2017), Trini et al. (2018), Veratti et al. (2020), Russo et al. (2021), Villani et al. (2021), Barbero et al. (2021)	Hamer et al., 2020	Belda et al. (2021), Maronga et al. (2019), (San José et al. (2021), San José and Perez-Camanyo (2022, 2023)	Horváth et al. (2016), Környei et al. (2021)

$$\mathrm{MFB} = \frac{1}{\mathrm{N}} \sum_{\mathrm{i}=1}^{\mathrm{N}} \frac{\mathrm{M_i} - \mathrm{O_i}}{(\mathrm{M_i} + \mathrm{O_i})/2}$$

3. Mean Fractional Error (*MFE*):

$$\mathrm{MFE} = \frac{1}{\mathrm{N}} \sum_{\mathrm{i}=1}^{\mathrm{N}} \frac{|\mathrm{M_i} - \mathrm{O_i}|}{(\mathrm{M_i} + \mathrm{O_i})/2}$$

4. Normalized Root Mean Square Error (*NRMSE*):

$$\mathrm{NRMSE} = \sqrt{\frac{\sum_{\mathrm{i}=1}^{\mathrm{N}} (\mathrm{M_i} - \mathrm{O_i})^2}{\sum_{\mathrm{i}=1}^{\mathrm{N}} \mathrm{O_i}^2}}$$

5. Ratio of predictions falling into a factor 2 ($0.5 \leq M_i/O_i \leq 2$) of the observations (*FAC2*).

M_i and O_i are the modelled and observed data i (concentration at hour or sampler i), respectively, and N is the number of data values. σ_M and σ_O are the sample standard deviations of model results and observations, respectively. The ideal value of R is unity, and the ideal values of *MFB*, *MFE* and *NRMSE* are all zero. *MFB*, *MFE* and *NRMSE* quantify the magnitude of the model error to some extent due to their dependence on '$(M_i - O_i)$'.

These metrics were applied for the monthly-averaged concentrations at sampler locations and for the spatial gradients of concentrations.

The spatial concentration gradients of NO_2 concentrations $\nabla C_{i,j}$ between pairs of samplers (i,j) have been computed by means of:

$$\nabla C_{i,j} = \frac{C_i - C_j}{d_{i,j}} \quad (1)$$

where C_i is the concentration at sampler i and $d_{i,j}$ is the distance between the samplers i and j. These gradients were computed for the measured data and for the modelling results and were compared both statistically and graphically. This comparison aims to investigate if the concentration distributions are appropriately reproduced by the modelling systems.

3. Results

Despite the main focus of the paper being to investigate how good are the model applications in estimating long-term average concentrations of NO_2 in an urban district, previously an evaluation of the models' performance simulating the hourly NO_2 concentration at the two air quality stations during one day of high pollution (see Supplementary material). In short, most of the model applications were able to simulate quite well the time evolution of NO_2 concentration along a day of relatively high pollution. Most applications underpredicted (especially in the early night peak), and some models failed to predict the timing of the concentration peaks. The model applications also seem to simulate background air quality station concentrations more accurately than those from the traffic station.

3.1. Monthly average data of NO_2 concentrations recorded by passive samplers

3.1.1. NO_2 concentrations at all samplers

Using a statistical approach to the comparison of NO_2 concentration data recorded by passive samplers for the campaign period (monthly average data) with modelled data (Fig. 3), the correlation coefficient (R) is higher than or equal to 0.70 for ten modelling applications, six

Table 2
Description of the models used for making scenario simulations for retrieving monthly average concentrations through scenarios-based approaches.

	VITO	CIEMAT	UOWM	SZE	AIR&D	AIR&D
Model	OpenFOAM	Star CCM+	ADREA-HF	OpenFOAM	OpenFOAM	FOLLOWAIR
Description	CFD – RANS steady state	CFD – RANS steady state	CFD – RANS steady state	CFD – RANS steady state	CFD – RANS unsteady state (time-average after convergence)	Encoder decoder Convolutional Neural Network (CNN) trained on CFD-RANS unsteady averaged results
Schmidt number (*Sc*)	0.5	0.3	0.7	0.5	0.7	0.7
Urban morphology	LOd1.2: 3D reconstruction based on building footprints and heights. Used CITY4CFD.	Data provided by VITO. Buildings simplified and grouped in blocks.	Data provided by VITO. No simplifications.			
Computational domain	Buildings: 1.5 × 1.5km2. Avg distance to boundary ~500 m	Buildings within a rectangle 1 km × 1 km. Distance from buildings to lateral boundaries = 8H; Height of domain = 8H; Hmax = height of tallest building	Buildings within 1 km × 1 km. The horizontal domain has been extended by 20 m in each for the four (4) sides flat with roughness 0.3 m. Vertical dimension 300 m	2.6 km × 2.6 km with buildings in AOI. 8.6kmx8.6 km total simulation domain. Height of domain = 400 m	Buildings within a rectangle 1.3 km × 1.3 km. Distance from buildings to lateral boundaries = 200 m; Height of domain = 358 m; Hmax = 70 m	Buildings within a rectangle 1.3 km × 1.3 km.
Grid type	Unstructured Polyhedral mesh. Build with SnappyHexMesh	Irregular. Polyhedral with hexahedral prism layers close to buildings and ground	Structured, irregular	Octree mesh with cell sizes from 2 to 32 m.	Regular. Unstructured. Cubical	Regular.
Grid resolution	Resolution at building level ~1 m	<1 m/>	Horizontal resolution uniform 5 m; NX = 204, NY = 204. Vertical resolution nonuniform; dz-min = 2.0 m, dzmax = 10.0 m;NZ = 60 m	2 m at ground level	0.5 × 0.5 m (proximity to walls) up to 16 × 16 m (for the highest altitudes)	Resolution of 1x1m^2
Total number of cells	19 million	1,180,000		3.3 million	12 million	
Emissions data	Computed using the FASTRACE model, and applying time profiles	Traffic emission data, together with the temporal profiles provided by VITO				
Chemistry	Passive scalar. NO_2/NO_x correction based on measurements	No chemistry. Passive scalar pollutant.			Passive scalar. NO_2/NO_x correction based on DERWENT and BACHLIN parametrizations	Passive scalar. NO_2/NO_x correction based on DERWENT and BACHLIN parametrizations
Atmospheric stability	Neutral atmospheric stability conditions.					
Meteorological boundary conditions	Data from the meteorological station: Antwerpen-Luchtbal.					
Pollution boundary conditions/ background concentrations	Background concentrations provided by RIO model.					
Assumptions and/or limitations	Concentrations proportional to 1/wind speed; Non-reactive pollutants; Thermal effects negligible; Concentration at a selected hour only depends on the emissions within the modelling domain, NO2/Nox ratio and meteorological conditions at that hour.	Concentrations proportional to 1/wind speed; Non-reactive pollutants; Thermal effects negligible; Concentration at a selected hour only depends on the emissions within the modelling domain and meteorological conditions at that hour.	Concentrations proportional to 1/wind speed; Non-reactive pollutants; Thermal effects negligible; Concentration at a selected hour only depends on the emissions within the modelling domain and meteorological conditions at that hour.	Concentrations proportional to 1/wind speed; Non-reactive pollutants; Thermal effects negligible; Concentration at a selected hour only depends on the emissions within the modelling domain and meteorological conditions at that hour.	Concentrations proportional to 1/wind speed (neutral assumption); Non-reactive pollutants; Thermal effects negligible; Concentration at a selected hour only depends on the emissions within the modelling domain, meteorological conditions at that hour and the background pollution model provided by the RIO model.	
References	Janssen et al. (2008), Vranckx et al. (2015), Sousa et al. (2018), Sousa and Gorlé (2019), Hooyberghs et al. (2022), Paden et al. (2022)	Rivas et al. (2019); Santiago et al. (2013, 2017, 2022); Santiago and Martin (2015), Sanchez et al. (2017); Parra et al. (2010)	(Bartzis et al. (2015, 2020a,b, 2021, 2022); Sakellaris et al. (2022)	Horváth et al. (2016); Környei et al. (2021)	Reiminger et al. (2020a, 2020b); Jurado et al. (2021)	Jurado et al. (2022)

Table 3
Description of methodologies involved in the model applications for retrieving monthly average concentrations in the case of scenarios-based approaches.

Institution	VITO	CERC-CIEMAT	CIEMAT detailed	CIEMAT simple	CIEMAT wind-factor	UOWM	AIR&D	AIR&D
Model	OpenFOAM	Star CCM+	Star CCM+	Star CCM+	Star CCM+	ADREA-HF	OpenFOAM	FOLLOWAIR
Set of simulations required/no. of scenarios	36 wind sectors scenarios	16 wind sector scenarios + wind speed bins from VITO met measurements + roadside & background pollutant concentration measurement	16 wind sector scenarios	16 wind sector scenarios	16 wind sector scenarios + wind speed bins	32 wind sector scenarios	18 wind sector scenarios	36 wind sector scenarios
Criteria for selecting scenarios	Measured wind direction (VITO meteorological data)	Measured wind speed, wind direction, and peak or off-peak traffic flows	Measured wind direction (VITO meteorological data)					
Procedure for retrieving annual/ monthly concentrations	Series of hourly concentration maps (gridded data) computed by assigning one scenario each hour and applying corrections by wind speed or by hour/date (emissions). NO2/NOx ratio per hour and adding background concentrations. Annual/monthly concentration maps estimated averaging for the time series of maps for a year/month	1) Derive wind-speed and traffic emissions correction factors from measured concentration data. 2) Calculate the frequency of occurrence of each wind speed/traffic emissions combination on a sector by sector basis (monthly/ annual). 3) Calculate weighted sum of 16 CFD gridded concentration maps	Series of hourly concentration maps (gridded data) computed by assigning one scenario each hour and applying corrections by wind speed or by hour/date (emissions) and adding background concentrations. Annual/monthly concentration maps estimated averaging for the time series of maps for a year/month	Weighted average based on probability density function (wind direction) + corrections by hour/date (emissions) and wind speed and adding background concentrations.	Weighted average based on probability density function (wind direction and wind speed scenarios) + corrections by hour/date (emissions) and wind speed and adding background concentrations.	32 Steady state reference simulations (i.e. one (1) per each sector) with wind velocity at the meteorological station 5 m/ s. These 32 simulations are utilized to estimate the 8764 h applying corrections by wind speed and by hour/ date (emissions) and adding background concentrations.	Series of hourly concentration maps (gridded data) computed by assigning one scenario each hour and applying corrections by wind speed or by hour/date (emissions) and adding background concentrations. Annual/monthly concentration maps estimated averaging for the time series of maps for a year/month	
Assumptions and/or limitations		Dependence of concentrations on wind speed and traffic emissions is spatially homogeneous; Influence of atmospheric stability on solution dependent through wind speed magnitude only; non-reactive pollutants; thermal effects negligible; concentration at a selected hour only depends on the emissions within the modelling domain and meteorological conditions at that hour.						

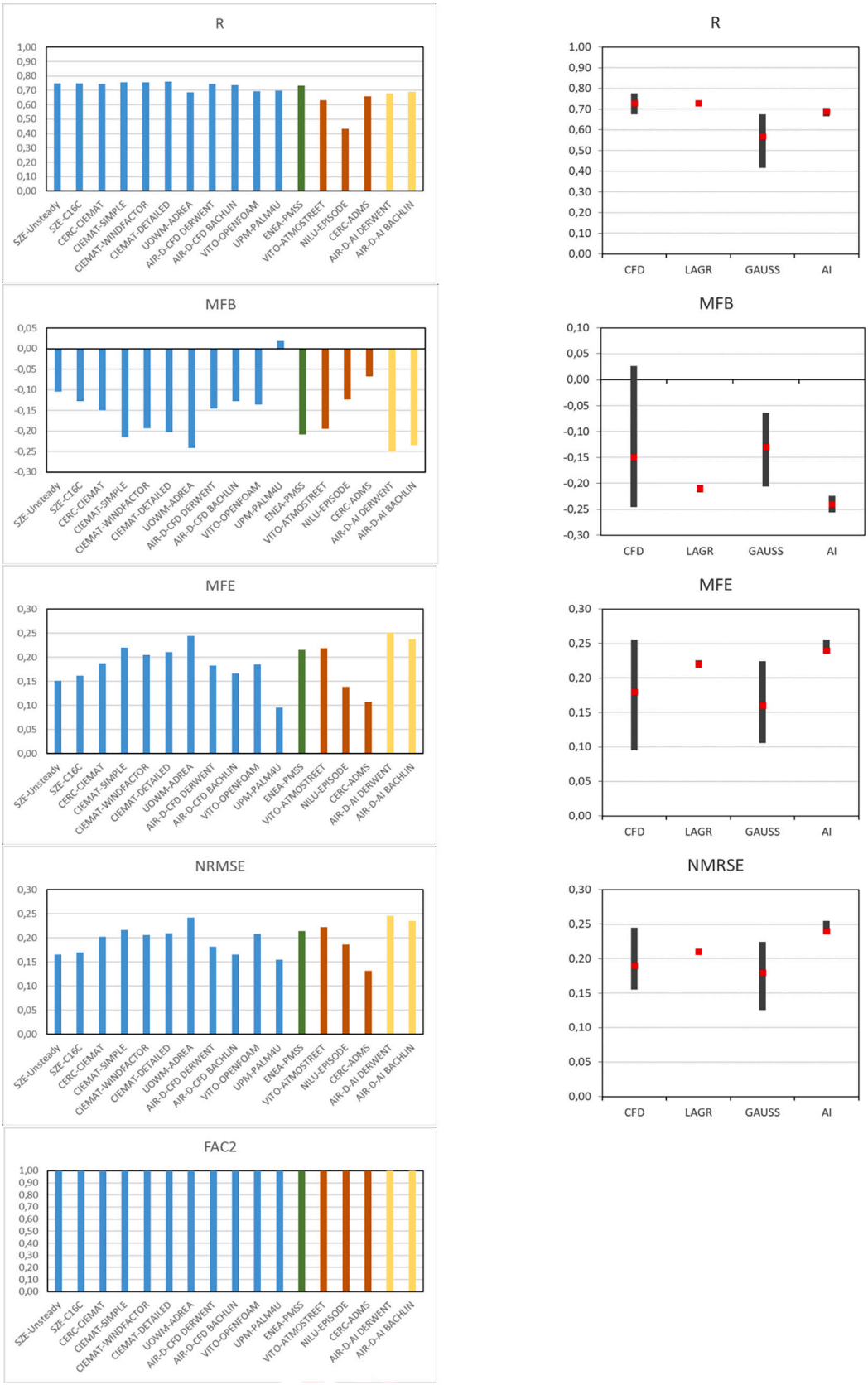

Fig. 3. Statistical results of R (Pearson correlation coefficient), MFB (mean fractional bias), MFE (mean fractional error), NRMSE (normalized root mean square error) and FAC2 (Ratio of predictions falling into a factor 2 of the observations) for the model predictions of average NO_2 concentrations at sampler points for the campaign period (April 30th to May 28th, 2016) for each model application (left, the blue colored bars refer to CFD models, green to the Lagrangian model, red to the Gaussian models and yellow to the AI models) and grouped by model types (right, the black bar is the range and the red squares mean value). CFD = Computational Fluid Dynamics, GAUSS = Gaussian models, LAGR = Lagrangian models, and AI = Artificial Intelligence models.

applications have an R higher than 0.60, and one model approach (NILU-EPISODE) has relatively low correlation (0.43). Most of the modelling applications underpredict slightly the monthly average concentration at sampler locations with MFB ranging between (−0.25 and −0.07), except UPM-PALM4U. Prediction errors are small (MFE and NRMSE ranging between 0.10 and 0.25). All models score FAC2 equal to 1 (Fig. 3). The resulting scores for MFB, MFE, and NRMSE are better for the monthly concentration average at sampler points than for the hourly time series at the air quality stations (see Supplementary material, SM1).

Analyzing the statistical metrics for the NO_2 concentrations by model types, the Gaussian models have R values lower than the other type of models and with a larger spread, which shows the importance in including street parameterizations and local meteorology; CFD, Lagrangian and AI model-based modelling applications provide better correlation coefficients, which indicates a better performance simulating the spatial variability of concentrations. The trend across statistical metrics for all models is broadly similar. In terms of the metrics that relate to the magnitude of the model error (MFB, MFE and NRMSE) all types of models show a similar trend, showing some underprediction (averages values of MFB −0.24 and −0.13) and averages MFE and NRMSE values lower than 0.24. All model applications have FAC2 close to 1.00.

These results are in agreement with the scatter plots of model predictions versus sampler measurements (Fig. SM2.1), which showed that the Gaussian models have the lowest regression slopes (<0.50, the extreme case is the NILU-EPISODE model with regression slope close to 0 as the only high resolution input taken into account is traffic emissions) in contrast with the other model types, which have higher regression slopes closer to 1.0, but mostly lower than 1.0.

3.1.2. NO_2 concentrations at all samplers of streets with and without emission data

One aspect rising of the analysis of the scatter plots of model predictions versus passive sampler measurements (Fig. SM2.1) is that all models have points of predicted low concentration when the measured concentration are not so low. These situations correspond to samplers (>60 %) that are located in streets for which there are no emission data. In fact, the emissions data is only covering main streets where results of the underlying traffic model are available and represent the only emission information available for models. Hence, it is important to compute separate statistical metrics for samplers located in streets with and without emission data, to evaluate the impact of emission data on simulated concentrations.

Fig. 4 clearly shows that the CFD, Lagrangian and AI models monthly average concentration statistical metrics at sampler locations improves very significantly only when data from samplers located in streets with emission data are used. These metrics worsen when only samplers from streets without emission data are considered. This behaviour does not seem to be detected for the Gaussian models, because buildings are inexistent or parameterized and the dispersion occurs to the further away streets without emission data.

3.1.3. Spatial gradients of NO_2 concentrations

The statistical metrics computed for the NO_2 concentration gradients between every pair of sampler points for the campaign period computed using Eq. (1) are shown in Fig. 5.

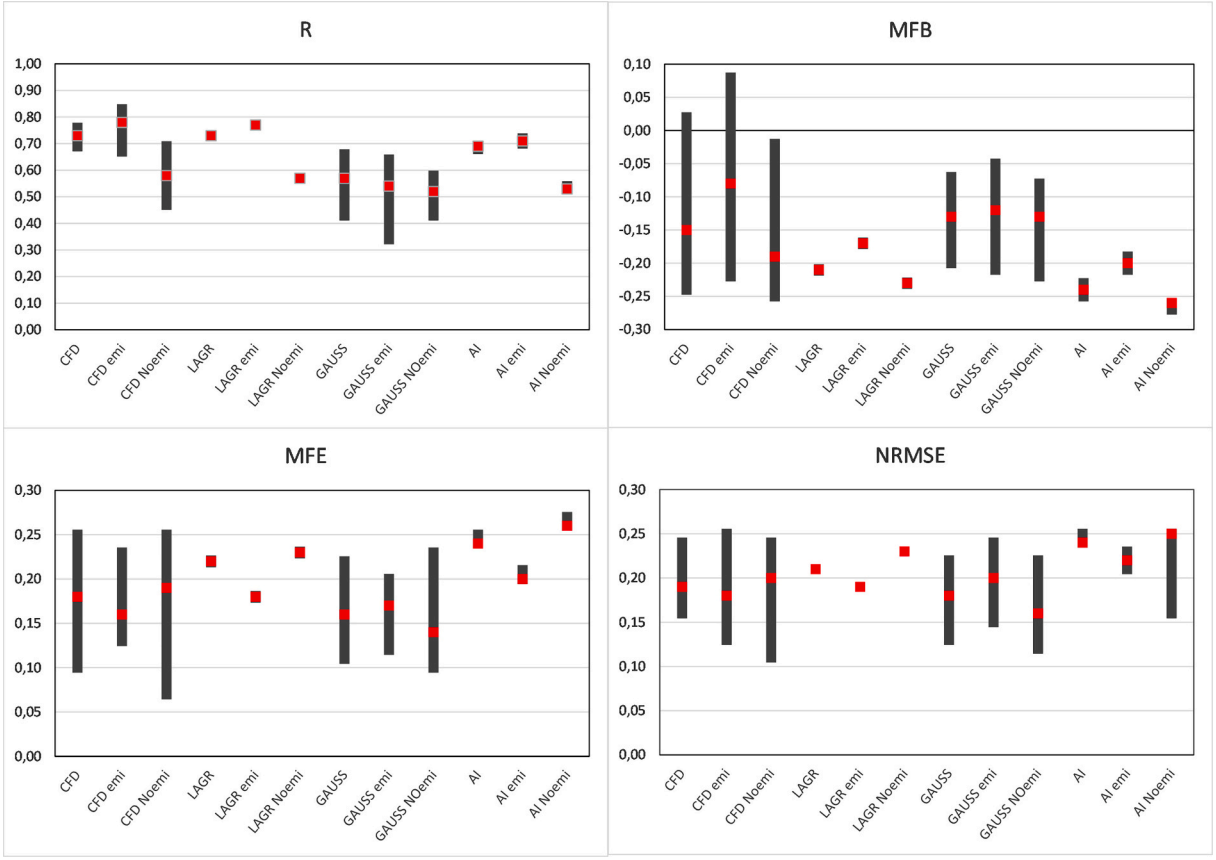

Fig. 4. Statistical results of R (Pearson correlation coefficient), MFB (mean fractional bias), MFE (mean fractional error), NRMSE (normalized root mean square error) and FAC2 (Ratio of predictions falling into a factor 2 of the observations) for the modelling applications predictions of average NO_2 concentrations at sampler points for the campaign period (April 30th to May 28th, 2016) for the different type of modelling applications using data from all the samplers, only from samplers located in streets with emission data (labeled EMI) and without emission data (labeled NOEMI). CFD = Computational Fluid Dynamics, GAUSS = Gaussian models, LAGR = Lagrangian models, and AI = Artificial Intelligence models.

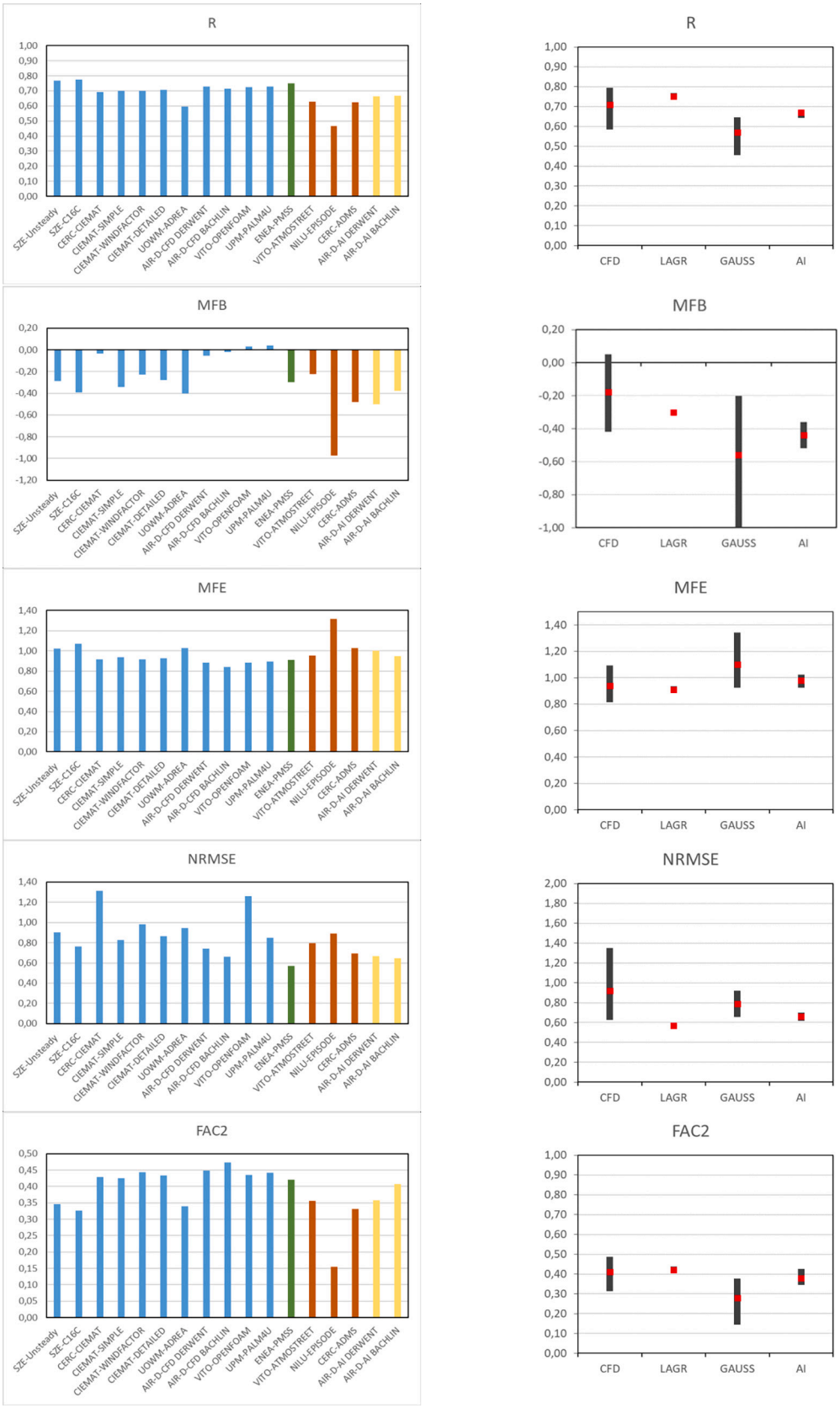

Fig. 5. Statistical results of R (Pearson correlation coefficient), MFB (mean fractional bias), MFE (mean fractional error), NRMSE (normalized root mean square error) and FAC2 (Ratio of predictions falling into a factor 2 of the observations) for the predictions of NO_2 concentration gradients between every pair of sampler points for the campaign period (April 30th to May 28th, 2016) for each model application (left, the blue colored bars refer to CFD models, green to the Lagrangian model, red to the Gaussian models and yellow to the AI models) and grouped by model types (right, the black bar is the range and the red squares mean value). CFD = Computational Fluid Dynamics, GAUSS = Gaussian models, LAGR = Lagrangian models, and AI = Artificial Intelligence models.

The correlation coefficient (R) is higher or equal to 0.70 for 10 modelling applications, while only the simplest configuration by NILU-EPISODE has $R < 0.50$.

VITO-OpenFOAM, UPM-PALM4U, AIR-D-CFD Derwent, AIR-D-CFD Bachlin, and CERC-CIEMAT have very small biases. In the case of CERC-CIEMAT this is because the hourly measurements from background and roadside air quality stations have been used to calibrate model results. The remaining modelling applications underpredict. Most of the methodologies have MFB between −0.50 and −0.20. However, the MFB of three modelling applications is lower than −0.40, they are AIR-D-AI-DERWENT, CERC-ADMS, and NILU-EPISODE with the minimum value of MFB (−0.98).

Concerning the error metrics, MFE values are higher than 0.80 with the highest value for NILU-EPISODE. Two modelling applications (CERC-CIEMAT and VITO-OPENFOAM) have NRMSE values higher than 1.00. Only ENEA-PMSS has a NRMSE value lower than 0.60. The remaining modelling applications have NRMSE values between 0.60 and 1.00.

FAC2 values are relatively low ranging from 0.16 (NILU-EPISODE) and 0.47 (AIR-D-BACHLIN, VITO-OpenFOAM, and UPM-PALM4U). The remaining modelling applications have FAC2 higher than 0.30. It is clear that models providing little spatial variability have worse statistical results.

When the capability of the different types of models simulating the concentration gradients is analysed, the CFD model-based modelling applications, AI and Lagrangian models clearly obtain the highest R values (higher than 0.67). The CFD models underpredict to the least extent with MFB equal to −0.18, while other models such as Gaussian or AI strongly underpredict the gradients on average (MFB of −0.56 and −0.44, respectively). The MFE values are <1.00 for all the modelling applications except the Gaussian models. However, the NRMSE values is lower than 1 for all models but several cases of the CFD models can reach NRMSE values higher than 1. The lowest corresponding to the Lagrangian models. The higher values of FAC2 correspond to the CFD, AI and Lagrangian model (Fig. 5). It is worth to note that these results relate to averages over model types, while for the Lagrangian, values are for only one – high performing – application.

In Supplementary material (Fig. SM2.2), the scatter plots of concentration gradients predictions versus sampler measurements gradients are shown. The slopes of the regression lines look rather similar to those of concentration scatter plots (see Fig. SM2.1). Seven modelling applications have a regression slope close to 1. Two applications (CERC-CIEMAT and VITO-OpenFOAM) have a regression slope higher than 1). The slope for eight modelling applications is lower than 1, some of them with slopes lower than 0.50 (CERC-ADMS) or even close to 0 (NILU-EPISODE). The maximum predicted gradient is higher than the observed maximum gradient for all modelling applications except for ENEA-PMSS and NILU-EPISODE. The last one especially underpredicts strongly the concentration gradients.

3.2. Monthly average NO_2 concentration maps

The monthly average NO_2 concentration fields computed by the diverse modelling applications and the measured data at the passive sampler locations are compared and their results are discussed in this section.

Nineteen samplers showed concentration values between 40 and 50 μg/m3. They had been placed close to the main thoroughfare of Plantin en Moretuslei (the main avenue crossing West to East by the center of the domain), especially in locations with stop signs (the driving conditions around stop signs are conducive to higher exhaust emissions), and at or close to several crossings at smaller streets to the North (see green squares in Fig. 6). Higher concentration hotspots, with monthly concentrations between 50 and 60 μg/m^3 are found at zone A at North (two samplers) and zone B in the center of the domain (four samplers).

It is important to point out that there were no emission data for the

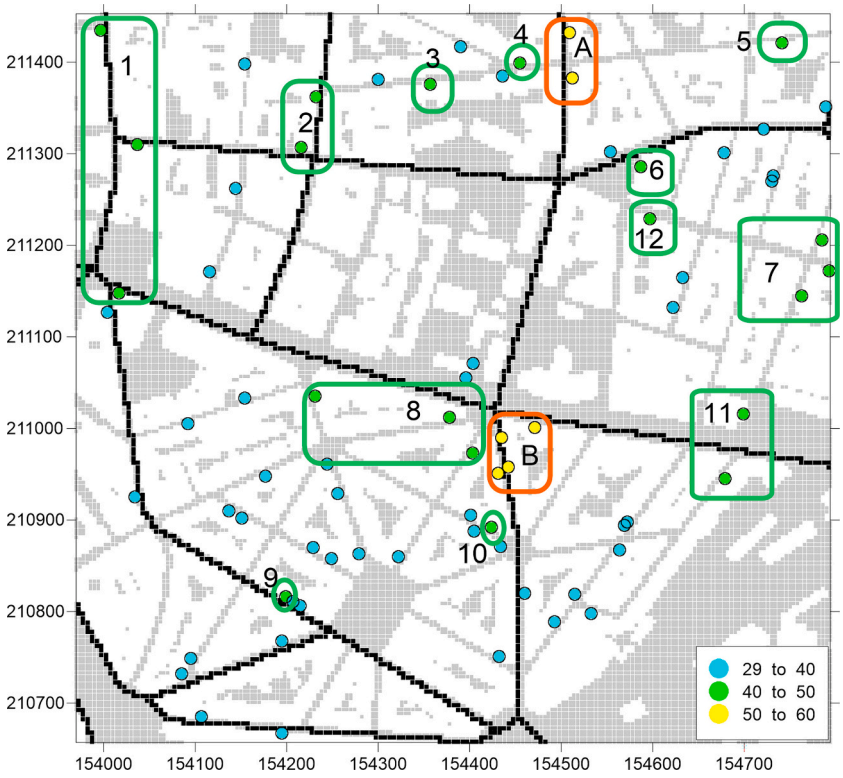

Fig. 6. Map showing the monthly NO_2 concentrations at each sampler point. The green rectangles and circles show the samplers with concentrations between 40 and 50 μg/m^{3}and the orange ones group the samplers with concentrations higher than 50 μg/m^3. Back lines show the streets, where emission data are available. White areas are buildings.

streets corresponding to the high NO_2 concentration samplers of zones 3, 4, 5, 7, 8, 10, and 12 (see Fig. 6). This is the main cause for all models underprediction of the NO_2 concentration at these samplers' locations. Therefore, the discussion about the performance of the models will be mainly focused on zones 1, 2, 9, 11, 6, A and B.

It is relevant to highlight that most of the models (especially the more complex ones) predict very high concentrations at the same places mainly along the main avenues and streets. Unfortunately, in some of these high-concentration areas, there were no samplers' measurements available. Nevertheless, there are few discrepancies between models as will be discussed later.

As shown in Fig. 7, the most basic modelling approach NILU-EPISODE using a Gaussian submodel, with a coarse modelled wind field and no building information, could only capture the hotspot area (concentrations above 40 μg/m3) at and around Plantin en Moretuslei (zones 8 and 11, and one sampler of zone 1 and another one of zone B) depicting the main road with the higher traffic emissions in the domain. All models agree that this road has high pollution levels. The other Gaussian models VITO-ATMOSTREET and CERC-ADMS, which account for the urban morphology could detect its effect on concentrations at zones 1, A, B, and some samplers of zone 11. For these zones, VITO-ATMOSTREET underestimated the passive sampler concentrations at samplers of zones 11, A, and B, but it overestimated at samplers of zone 1. CERC-ADMS was able to simulate well the hotspots of zones 1, 11, A, and B, but it overestimated most of the samplers of zone 1.

CFD models explicitly calculate the airflow within the 3D urban structure and thus can provide detailed results within the street as we can see from the monthly mean NO_2 concentration gradients in Fig. 8. The maps of the concentration predicted by the CFD models are quite similar but with some differences in the location and intensity of some high-concentration zones. For example, in zone 1, almost all models overpredict, except UOWM-ADREA, which underpredict in some samplers, or CERC-CIEMAT and CIEMAT, which fit quite well the observations here. Zone 6 is not well predicted by most of the CFD models. Except for SZE-C16C (SZE, 16 wind direction scenarios CFD simulations) and CIEMAT that can reproduce a hotspot in the beginning of the street and then do not overestimate along the street. Zone B is mostly overestimated by the majority of the CFD models, but to a lesser extent by CIEMAT.

The CFD models mostly underestimated Zone A, but AIR-D and UOWM predicted it quite well. Zone 2 is well predicted by SZE-unsteady, VITO-OPENFOAM, and AIR-D, whereas most modelling applications underpredict. There is mostly underestimation in zone 9. However, in zone 11, several models estimate correctly the concentration (UPM, AIR-D, VITO-OPENFOAM, and to a lesser extent CIEMAT, CERC-CIEMAT, and SZE-unsteady).

The long-term CFD unsteady simulation (SZE-Unsteady) map has been selected as a reference map since no statistical post-processing was applied to derive the monthly or annual mean. Maps from the other modelling applications have features consistent with those of the unsteady simulation. The maps from CIEMAT-DETAILED, CERC-CIEMAT, and SZR-C16C seem to be more similar to the SZE-unsteady map. Most of the high-concentration areas in SZE-unsteady are predicted by all models. However, there are also some high concentrations inside some secondary streets which are not predicted by all models. The values of the maximum concentrations are significantly different among the models. In contrast with the Gaussian models, the CFD models (also the Lagrangian and AI models) simulate the inhomogeneity in terms of the buildings that form street canyons. The maximum concentrations at the streets are shifted to the upwind sidewalks (due to the street-canyon vortex), and they predict lower concentrations at street crossings (due to higher ventilation). It is important to highlight the variability of the magnitude of the predicted higher concentration among the different maps. For example, UPM-PALM4U, VITO-OpenFOAM, and especially UOWM-ADREA predict much higher concentrations in some areas.

The Lagrangian model with CFD simplified meteorology ENEA-PMSS results show a spatial distribution that is very similar to the CFD models' results, with the highest concentration in almost the same zones, but with overall lower concentrations (Fig. 9). This model underestimates concentrations at several sampler locations of zones A, B, 1, 2, 6, 9, and 11, but it overestimates in one sampler of zone 1 right located at the main W-E avenue. The prediction is correct in one sampler of zone B located at the main avenue, and another one of zone 11.

The AI results also show a quite similar distribution to the CFD models, with similar or higher concentrations. The AI models predict quite well the zone 1, but they overpredict at the southern sampler (like most of the models do). On the contrary, the concentration at the samplers of zones A, B, 2, 6, and 11 are mostly underpredicted.

The concentration estimated using the DERWENT parameterization accounting for NO_2/NOx ratios is very similar to the maps when the BACHLIN parameterization is used. The same happens with the AIR-D-CFD simulations using both parametrizations (Fig. 10).

3.3. *Evaluation of long-term simulations versus and modelling applications based on a limited number of scenarios*

The SZE group made an unsteady CFD RANS simulation for all the campaign period (April 30th-May 28th, 2016) for NO_2. Additionally, SZE, UOWM, VITO and CIEMAT groups computed the NO_2 concentration using a methodology based on steady CFD-RANS simulations of wind direction sector scenarios corresponding to 4, 8, 16, 32 and 36 sectors, but not all groups covered all of them (Table 4). The aim of this analysis is to assess differences in scenario-based results deviating from those of the long-term unsteady simulation.

In this section, the results of the comparison of all these simulations for the monthly (April 30th-May 28th, 2016) NO_2 concentrations (and concentration gradients) with data recorded by the passive samplers deployed in the modelling domain were analysed in order to answer the

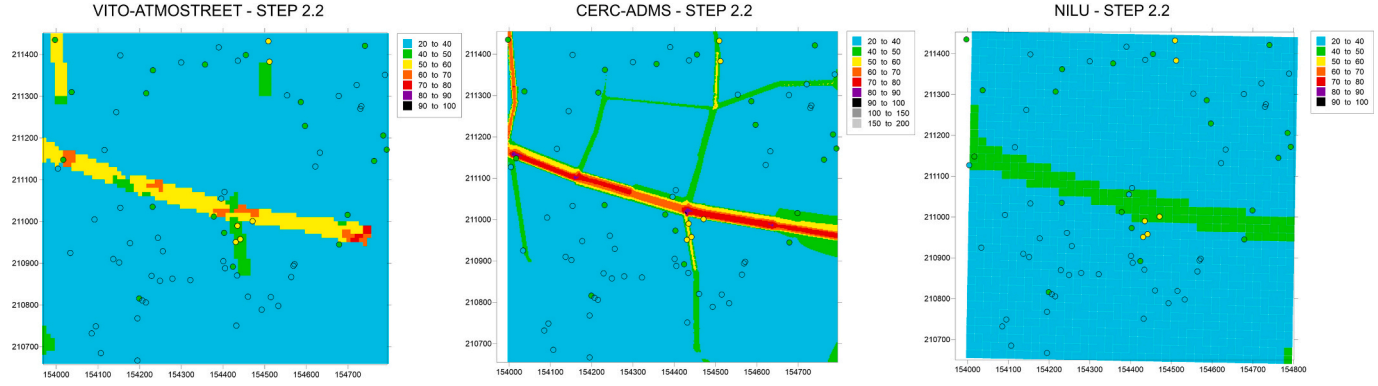

Fig. 7. Maps of the monthly average NO_2 concentrations (μg/m^3) for the three Gaussian models and concentrations measured by passive samplers (colored dots).

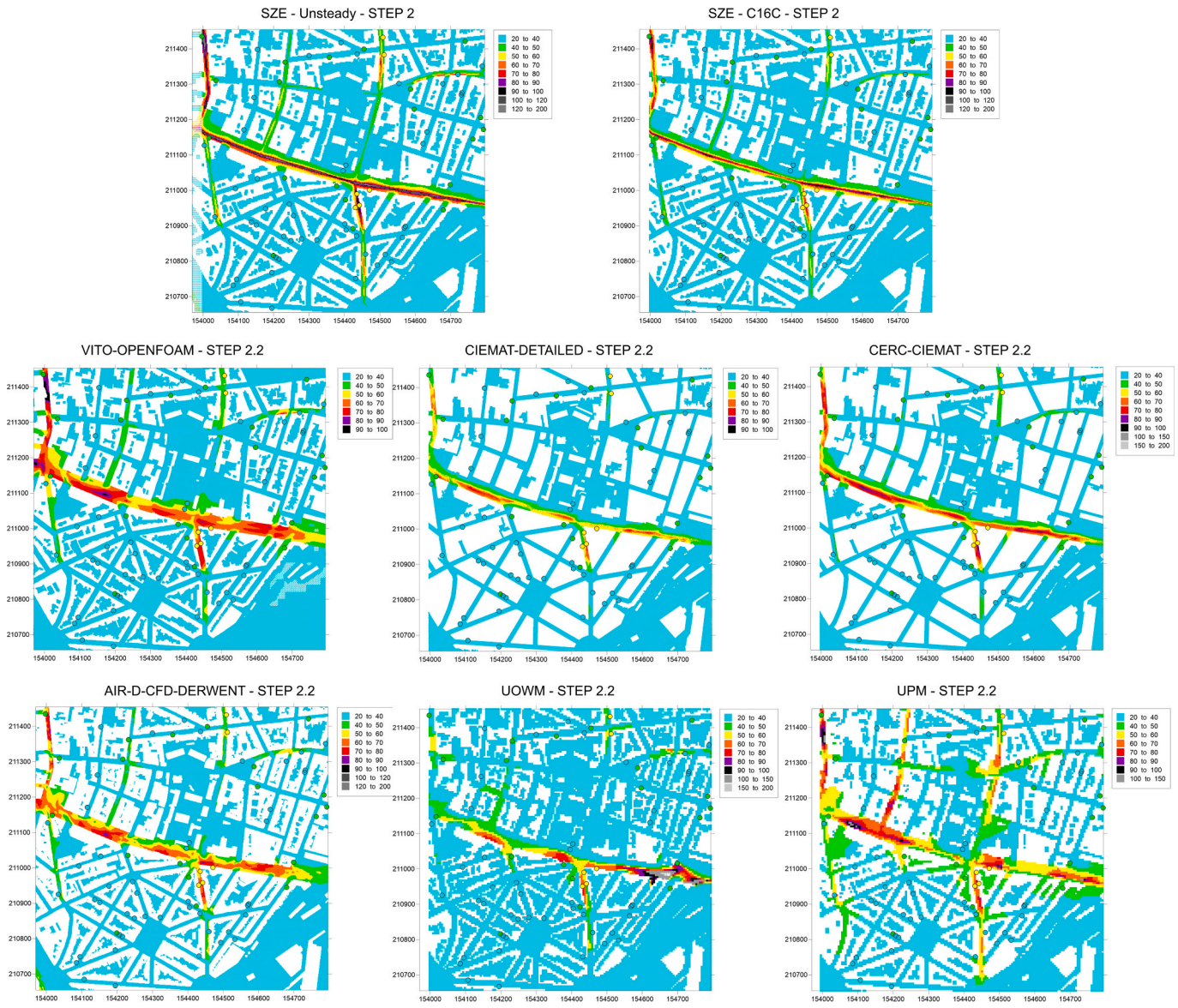

Fig. 8. Maps of the monthly average NO_2 concentration (μg/m^3) for the long-term CFD unsteady simulation (upper left) and for eight modelling applications based on scenario CFD simulations and concentration measured by passive samplers (colored dots).

following questions:

1) How good are scenario-based modelling applications in comparison to long-term simulations?
2) How many scenarios are needed to get results similar to long-term simulations in dense urban areas?

The results are shown in Fig. 11.

For the SZE-OpenFOAM unsteady simulation. The values of metrics for NO_2 concentration prediction are similar to the SZE-OpenFOAM modelling application based on scenario simulations for FAC2 and MFE, whereas the metrics are clearly better for MFB (slight under-prediction), and a little bit worse for R and NRMSE. In the case of the NO_2 concentration gradients, the FAC2 is very similar for the SZE-OpenFOAM unsteady simulation and the SZE-OpenFOAM modelling application, while for R and MFE the unsteady simulation provides slightly worse results and more clearly worse for MFB (increasing the overprediction) and NRMSE.

Analyzing the differences when using different number of scenarios, in the case of SZE, correlation coefficients change very little with the number of scenarios for the sampler's concentrations and concentration gradients. The MFB values for concentrations are very similar regardless of the number of scenarios. However, for concentration gradients the MFB changes following roughly a parabolic curve with a minimum around the 16-scenarios case, but with very similar MFB values to those obtained for the 8- and 32-scenario cases. MFE values do not seem to vary significantly with the number of scenarios. NRMSE has similar values for all scenario cases for concentrations, but for concentration gradients, NRMSE values are worse for 4-scenario case than for the others. FAC2 values are 1 (the maximum possible value) for all cases for NO_2 concentrations. However, for the NO_2 concentration gradients, there is some variability depending on the number of scenarios. Best values are for 16 and 32 scenarios.

Concerning the UOWM results, the correlation coefficients also change very little with the number of scenarios for the NO_2 concentrations and concentration gradients. Very little differences of the MFB values (for concentration and gradients) and MFE and NRMSE (only for concentrations) are detected for the UOWM, while for the MFE and NRMSE values for the concentrations gradients slightly improve as the number of scenarios increases. For the NO_2 concentration gradients, the

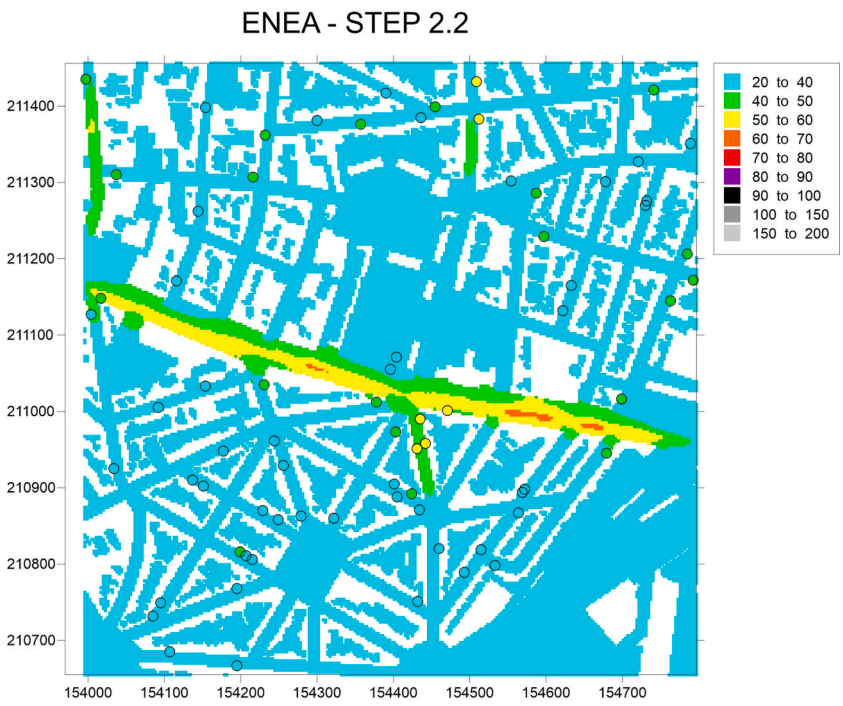

Fig. 9. Map of the monthly average NO_2 concentration (μg/m^3) for the ENEA-PMSS model, and concentration measured by passive samplers (colored dots).

best values of FAC2 are for 16 and 32 scenarios.

Referring to CIEMAT estimates, correlation coefficients for concentrations and concentration gradients increase with the number of scenarios, with a more significant change from 4 to 8 scenarios when NO_2 concentrations are considered. In spite of little differences of the MFB values being detected, there is a clear decrease of the overprediction of concentration gradients when the number of scenarios increases. The MFE values clearly decrease as the number of scenarios increases, but for the concentration gradients the minimum of MFE is for the 8-scenario case with a similar value when 16 scenarios are used. There is a clear improvement of NRMSE when the number of scenarios increases (the best for 16 scenarios) and also of the FAC2 values for concentration gradients but not so strongly.

With respect to VITO cases, correlation coefficients decrease as the number of scenarios increases up to 16 scenarios and keep similar values for 32 and 36 scenarios. The underprediction of NO_2 concentrations and gradients seems to be minimum when 32 scenarios are used. Additionally, the best MFE and NRMSE values for VITO also seem to be for the 32-scenario case for concentrations and concentration gradients, but very similar to the results for the 4-scenario case. However, for concentration gradients, the NRMSE values are slightly better for the 4-scenario case. Finally, the worst FAC2 values for the NO_2 concentration gradients are obtained for 16 and 36 scenarios and the best is for four scenarios.

4. Discussion

4.1. What is the impact of the emissions data?

The statistical metrics for the CFD, Lagrangian, and AI models (but not for all the Gaussian ones) improved notably when only data from samplers located at streets where emission data were available, whereas clearly worse for the samplers without emission data (see Section 3.1.2. Fig. 4). It is a very coherent performance. As expected, this analysis confirms that the lack of emission data in some streets has a relevant influence on the results of CFD, Lagrangian and AI modelling applications. For Gaussian models, the dispersion from line sources is still depicted in far away points of the streets, as buildings are not included or parameterized weakening the differences. Gaussian models rely extremely on the high resolution of road emission data to depict the spatial distribution of NO_2 concentrations and their challenge is how to include the effect of buildings on meteorology and dispersion. For models with detailed building information and their effects on meteorology and pollutant dispersion, further work on providing very detailed emission data both at spatial and temporal resolution is essential to provide better results in terms of long-term air quality predictions at microscale.

4.2. What type of modelling applications are more suitable to simulate the spatial distribution of long-term averaged NO_2 concentrations in complex urban morphology?

Most of the model applications were able to simulate quite well the time evolution of hourly NO_2 concentration along a day of relatively high pollution, but underpredicting peaks and sometimes their timings. Best predictions are for the background air quality station concentrations more accurately than those from the traffic station, mainly because background from the RIO model already partially account for the observations at the background station (see Supplementary material SM1).

Although the analysed methodologies generally underpredict the monthly NO_2 concentration, the spatial distribution of monthly NO_2 concentration is quite well simulated by many methodologies, but there are important differences. Concerning statistical metrics for modelled concentrations, Gaussian models have the best statistical results in terms of magnitude of error, followed by CFD then Lagrangian and AI. However, CFD and Lagrangian have the best correlation coefficients, followed by AI and then Gaussian (see Fig. 3).

Urban areas show very significant gradients of pollutants emitted from traffic such as NO_2. The data from the samplers deployed along this domain have shown that some gradients could be higher than 0.4 μg/m^3/m, which means that in the case of a 50 m wide street, the difference of concentration could be up to 20 μg/m^3 or more between both street sides. Hence, it is very important that the model be able to estimate the concentration gradients well in order to provide a reliable spatial distribution of pollutant concentration, allowing for a better air quality assessment.

In terms of statistical results for concentration gradients, the

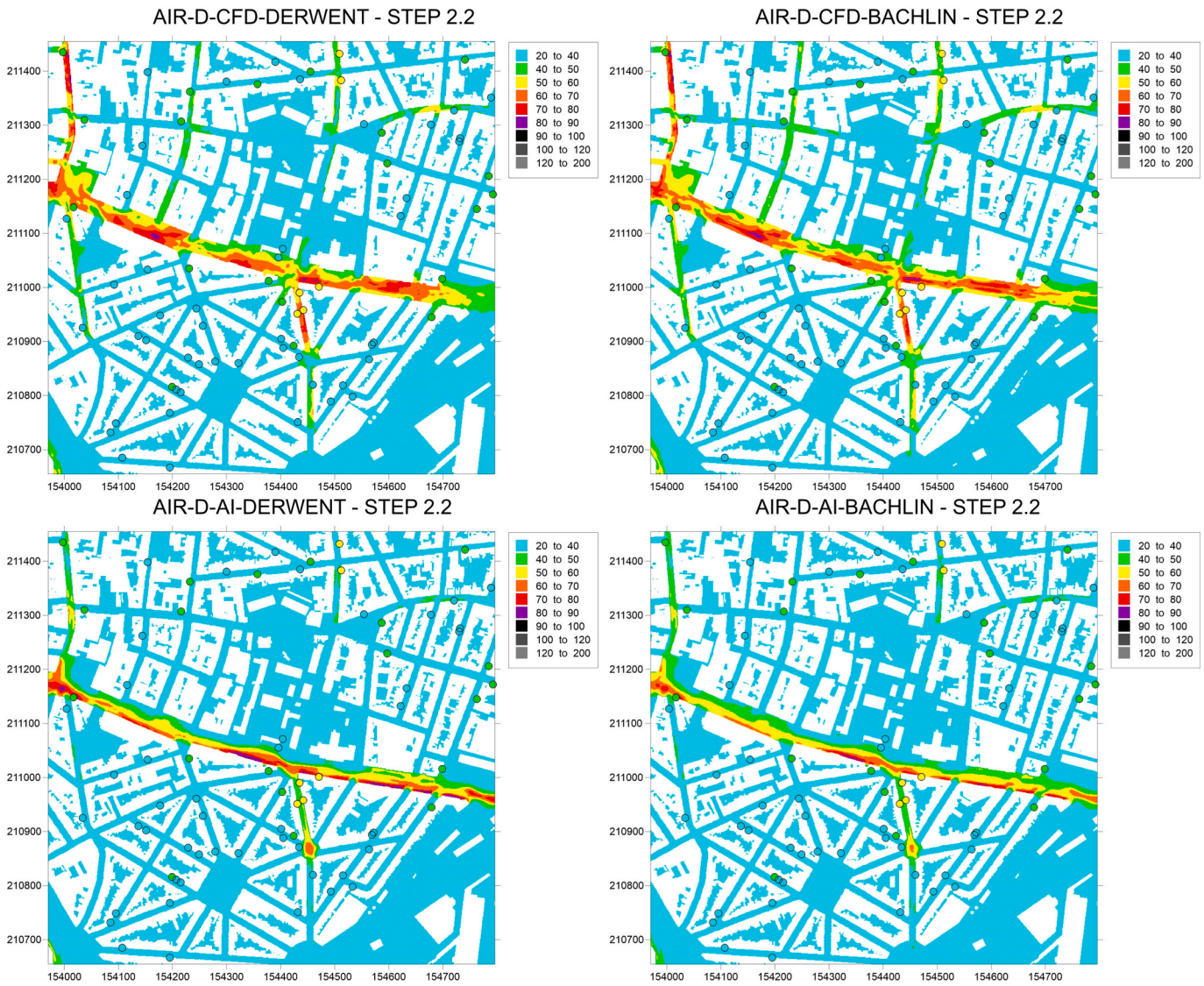

Fig. 10. Maps of the monthly average NO_2 concentration ($\mu g/m^3$) for the AIR-D-CFD (upper) and AIR-D-AI (lower) for the Derwent (left) and Bachlin (right) parametrizations accounting for the NO_2/NOx ratios and concentration measured by passive samplers (colored dots).

performance of the models varies with the metrics, e.g., CFD, Lagrangian and AI applications perform better in terms of FAC2, MFE and R, CFD applications have the better values of MFB, while the worst in average for the NRMSE (Lagrangian and AI show the best values of this metric). The CFD models, and to some extent the Lagrangian and AI models, are able to simulate rather well the spatial variation of pollutant concentrations both along and across street canyons (Fig. 5).

It is noteworthy that some streets with minimal traffic flow can nonetheless exhibit elevated pollutant concentrations in some cases. This counterintuitive phenomenon is attributed to local aerodynamic effects and specific wind patterns, such as vortices generated within street canyons, which can effectively trap pollutants. These dynamics may underscore the complexity of microscale dispersion and the potential for significant pollution levels in areas with low vehicular volume due to topographical and meteorological influences that confine pollutants to a restricted space.

The Gaussian models do not seem to have so good statistical results for concentration gradients. It is because they estimate much smoother concentration fields with low variability inside the streets, underestimating the concentration gradients, especially in the case of the simpler Gaussian model configuration (by NILU-EPISODE, with only emissions at high resolution and no adjustment for buildings or building morphology). Similar results were found by other authors in other studies (Pullen et al., 2005, Bady, 2014, Tripathi et al., 2018, Haeger-Eugensson et al., 2021 among others). Nevertheless, the Gaussian models with street-canyon parameterizations are able to detect hotspots and simulate strong across road variations (CERC-ADMS or VITO-ATMOSTREET models) having better statistical metrics than the NILU-EPISODE model. However, they do not simulate well along-road variability associated with changes in building density because individual building geometries are not accounted for by the models as can be seen in the results of the concentration maps of Section 3.2 (Figs. 7–10).

Some models (UPM, CERC-ADMS and NILU) that account for more complex chemistry processes provide a more accurate prediction of concentrations at the lower concentration range (see Supplementary material SM2). In general, the scatter plots indicate that the majority of the modelling applications underpredict the monthly average concentration. There are several possible explanations for the model underprediction of NO_2. In this comparative analysis, background concentrations were derived using two distinct methodologies across the evaluated models. Some models incorporated NO_2 background levels directly from the RIO model outputs. In contrast, other models harnessed nitrogen oxides (NO_x) background levels from the RIO model, subsequently converting these to NO_2 through a dedicated chemical

Table 4
Group, model and number of wind direction sectors used for computing average NO_2 concentrations for the campaign period (April 30th to May 28th, 2016).

Group/model	Number of wind direction sector scenarios
SZE OpenFOAM	4, 8, 16, 32
UOWM ADREA	8, 16, 32
VITO OpenFOAM	4, 8, 16, 32, 36
CIEMAT STAR CCM+	4, 8, 16

module. The direct use of NO_2 background data from the RIO model resulted in reliable estimates of the minimum pollution levels as measured by the samplers. On the other hand, utilizing NO_x as a precursor and processing it to NO_2 via the chemical module provided a robust approximation of the mean values within clusters of samplers marginally affected by emissions. This methodological divergence presents challenges in model comparison, particularly at lower concentration values, due to differing underlying assumptions regarding background concentration definitions and values (i.e., the smallest observed value versus the average of clustered low values). In addition, in this study, the results of the AIR-D (CFD and AI) models using the Derwent and Bachlin parametrization of the NO2/NOx ratio are not significantly different (Fig. 10). A specific study for investigating the importance of NO2 chemistry at microscale for improving estimates of long-term averaged NO2 concentrations is needed.

Despite all the CFD models used being RANS-type, the differences among the results seem to be relatively significant. These differences can be due to particular features of each model simulation or related to the long-term averaging method of the scenario cases. This means differences related to the particular processing of the emission input data, the type of selected scenarios, the post-processing of the scenarios simulations for retrieving long-term average concentrations, or the configuration of the specific CFD simulations of every scenario. To understand better the causes of the differences, a dedicated detailed study is needed, and this is now beyond the scope of this paper.

From this analysis, we conclude that the models that account for the full complexity of urban morphology and the involved atmospheric flows predict a more realistic spatial distribution of the NO_2 concentrations. In this sense, modelling applications based on CFD data and Lagrangian model seem to be suitable for an accurate simulation of the spatial variability of long-term averages of air pollutant concentrations. The modelling applications based on artificial intelligence trained with CFD simulations have also quite encouraging good results. However, Gaussian models that parameterise urban morphology generate comparatively simplistic representations of in-street concentration variations. They could be improved by including better parameterizations of the effects of buildings and streets on pollutant dispersion. CFD models could be also improved by better accounting for meteorological variations and atmospheric chemical reactions of the pollutants. Other options to be further explored in the future include coupled modelling systems.

4.3. Long term simulations versus modelling applications based on a limited number of scenarios

As said before, there two important questions:

1) How good are scenario-based modelling applications in comparison to long-term simulations?
2) How many scenarios are needed to get results similar to long-term simulations in dense urban areas?

With respect to the first question, in general modelling applications based on wind direction sector scenarios using the same model (SZE-OpenFOAM) provide results of comparable quality to those of as the SZE unsteady simulation (Fig. 11).

Concerning the second question, the statistical metrics for the results provided by the different groups do not agree completely, which makes it challenging to determine how many scenarios are required to have optimal results (Fig. 11). In the case of the SZE results, there are small differences on the performance in function of the number of scenarios, although using 16 or 32 scenarios leads to slightly better results. The UOWM results seem to be slightly more sensitive to the number of scenarios than SZE results and show somewhat better results when 16 or 32 scenarios are used. However, the CIEMAT results are the most sensitive to the increasing of number scenarios. Overall, eight or more wind direction sector scenarios demonstrates the best performance. Finally, in the case of the VITO simulations, the results seem to be not conclusive because for some metrics the best results are for 32 or 36 scenarios (MFB, MFE) but for others (R, NRMSE and FAC2) the best ones are for the case of only 4 scenarios. Although, all statistical results are rather similar regardless of the number of scenarios.

In general, there are small differences in the performance of scenario-based methodologies in function of the number of scenarios. Nonetheless some of the modelling approaches appear to give slightly better results when eight or more wind direction sector scenarios are used although the trends are modelling application or model dependent.

Nevertheless, it is unclear to what extent these conclusions can change with other types of urban morphology. Jurado et al. (2021) carried out a similar study for an urban district of a city of France aiming to find the minimum number of wind directions required to be simulated to accurately estimate annual averaged concentrations based on CFD results. They considered two approaches: one using wind direction sectors evenly spaced (the same approach used in this study), and another considering predominant wind directions. They found that the first approach is better on average and a limited number of wind direction scenarios (at least, six or nine) could be enough to obtain good estimates of annual mean concentrations with low computational cost. However, they concluded that it could depend on the building layout and wind-rose. Surely, more studies in other types of urban areas are necessary to reach more consistent conclusions.

5. Conclusions

An intercomparison exercise of modelling applications for computing long-term average of NO_2 concentrations in urban districts with a very high spatial resolution was performed under the framework of the Forum for Air Quality Modelling in Europe (FAIRMODE). This exercise involved modelling of a district of Antwerp (Belgium). Air quality data from two monitoring stations recording hourly concentrations, and 73 passive samplers recording the NO_2 monthly average concentrations deployed in the district for a month in 2016. The modelling domain was a square of 800×800 m^2. Nine modelling teams participated in this exercise providing results from 15 different methodologies based on different kinds of models (CFD, Lagrangian, Gaussian, and Artificial Intelligence). The majority of models used scenario-based approaches, which consisted of simulating representative scenarios and then applying a processing for retrieving a one-month average of NO_2 concentrations. The less computational intense models calculate predictions of hourly concentrations, which are then averaged over the month period. Additionally, an unsteady CFD simulation for the full month was carried out.

In the following lines, the main findings of this study are summarized.

Most of the model applications were able to simulate quite well the time evolution of NO_2 concentration along a day of relatively high pollution, but underpredicting some concentration peaks.

Although the analysed model applications generally underpredict the monthly NO_2 concentration, the spatial distribution of monthly NO_2 concentration is quite well simulated by many methodologies, but there are important differences especially evident in the performance predicting the concentration gradients. Model applications involving CFD

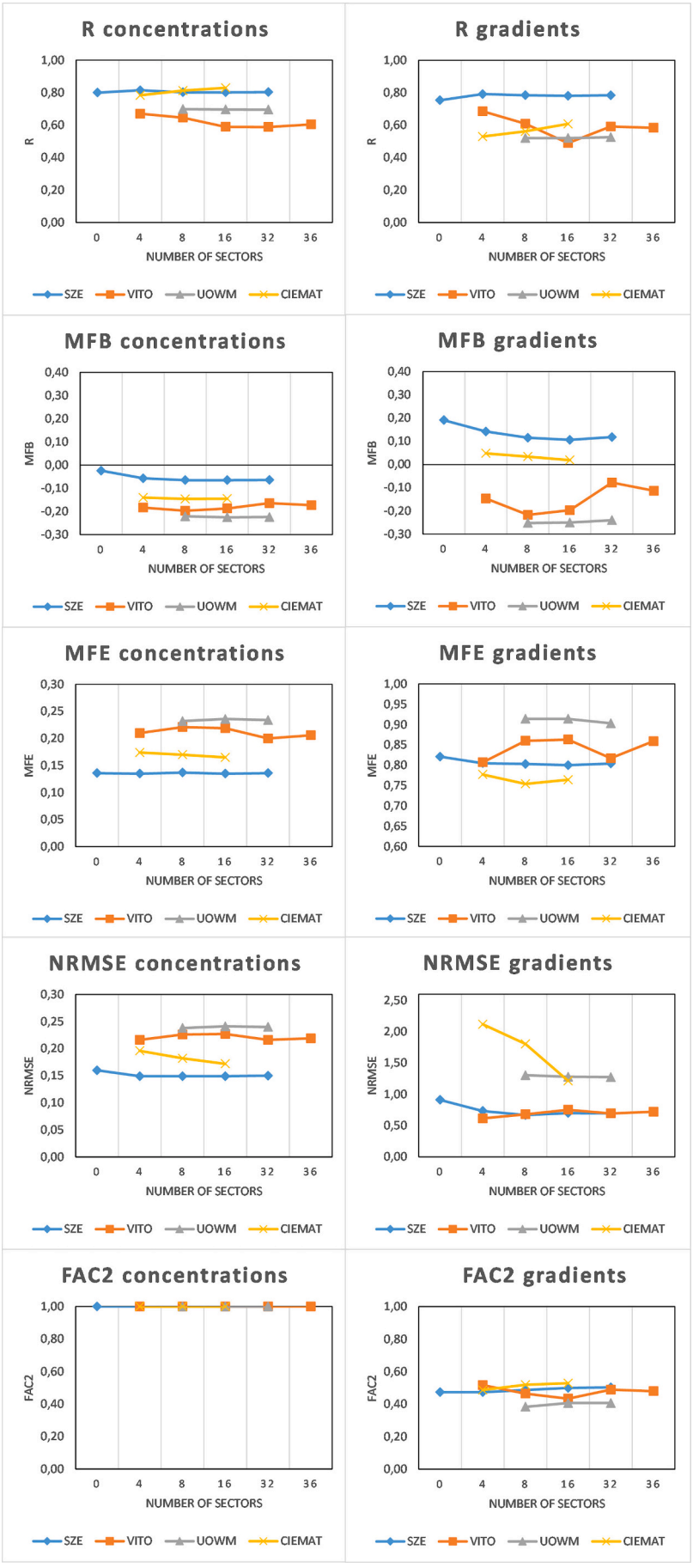

(caption on next page)

Fig. 11. Statistical results of R (Pearson correlation coefficient), MFB (mean fractional bias), MFE (mean fractional error), NRMSE (normalized root mean square error) and FAC2 (Ratio of predictions falling into a factor 2 of the observations) for the model predictions of average NO_2 concentrations (left) and gradients (right) at the passive sampler locations for the experimental campaign (April 30th-May 28th, 2016) for the SZE, VITO, UOWM and CIEMAT simulations for different number of wind direction sector scenarios and for the long-term unsteady simulations (labeled as 0 scenarios).

or Lagrangian or AI modelling trained with CFD simulations are able to simulate better the very notable spatial gradients of NO_2 concentration inside the streets. In contrast, the simpler Gaussian models provide smoother concentration fields underpredicting the concentration gradients. This is much less notable in the case of the Gaussian models, which include parametrization representing the effect of the street-canyons on flow and dispersion.

Any modelling study that generates air pollution maps at very high spatial resolution gives the illusion that the modelled concentrations are accurate at that level of detail. Detailed modelling should be presented alongside evaluation using measured data. Also, the resolution of emissions data should be consistent with the resolution of the outputs. The lack of emission data in some streets has a relevant influence on the CFD, Lagrangian and AI model applications' results and less for the Gaussian ones. This study has highlighted the need for good and detailed pollutant emission data resolution traffic, covering all the streets (not only the main ones), in order to obtain accurate simulation of pollution in urban hot spots at the microscale.

It seems that some models considering NO_2 chemistry provides better results for low concentration, but there were not important differences when different NO_2/NOx parametrizations were used with the same model. The impact of chemistry at microscale for improving estimates of long-term averaged NO_2 concentrations is a question for further research.

It is important to underline that some methodologies using a limited number of CFD simulated scenarios (wind direction scenarios) provide quite similar monthly NO_2 maps to those obtained with the long-term CFD unsteady simulation. Additionally, there are only small differences in the performance of scenario-based methodologies depending on the number of scenarios, although some methodologies give slightly better results when eight or more wind direction sector scenarios are used. Nevertheless, these results may depend on the urban area under study, and hence, more studies in other types of urban areas are needed. The authors are keen to undertake additional studies to deepen understanding of the detected differences observed in the results obtained with quite similar methodologies based on similar CFD models.

Given that the complexity of the models is associated with their ability to account for the full complexity of urban morphology and the associated atmospheric flows, we can conclude from the results of this study that the more complex the model, the more realistic the predicted spatial distribution of NO_2 concentrations appears to be. The results show simple Gaussian models without including any parametrization of the street canyon phenomena must not be used for a detailed analysis of the long-term NO_2 concentration distribution in urban districts. Advanced Gaussian models that include the effect of buildings on wind flow can be used to detect quite efficiently streets with hot spots. However, they have some limitations in terms of predicting the detailed spatial distribution of NO_2 concentrations within the streets, despite they seem to perform relatively well in terms of simulating hourly time series in the air quality stations locations. The more complex models (mainly CFD based methodologies, Lagrangian, or AI models) seem to provide better estimates of the spatial distribution of one-month averages of NO_2 concentrations. Overall, the CFD models seem to provide the best results. Approaches based on steady CFD-RANS model simulations (with their relatively minimal computational costs) of meteorological scenarios (different wind direction sectors) seem to provide good results, of similar quality to the results obtained with the unsteady CFD-RANS simulation (very high computational cost) for the complete one-month period.

This type of study is very relevant in order to determine what type of modelling applications could be best suited for detecting hotspots and getting a good estimate of the complex distribution in urban districts, which is very important for air quality assessment (determining the area of exceedance of air quality standards). Pollution maps generated from detailed AQ models, which have been evaluated using measurement data, are of use to local policy makers when considering options for addressing pollution hotspots issues including planning for air pollution abatement. In this sense, one of the applications of the best microscale model applications is to simulate scenarios for rearranging the traffic to reduce the air pollution in urban hot spots. Some studies applying CFD models can be found in the literature such as Parra et al. (2010), Santiago et al. (2017), Rivas et al. (2019) or Santiago et al. (2022).

CRediT authorship contribution statement

F. Martín: Writing – review & editing, Writing – original draft, Visualization, Validation, Supervision, Software, Resources, Project administration, Methodology, Investigation, Formal analysis, Data curation, Conceptualization. **S. Janssen:** Writing – review & editing, Writing – original draft, Supervision, Resources, Project administration, Methodology, Investigation, Formal analysis, Conceptualization. **V. Rodrigues:** Writing – review & editing, Writing – original draft, Supervision, Resources, Project administration, Methodology, Investigation, Formal analysis. **J. Sousa:** Writing – review & editing, Software, Resources, Methodology, Investigation, Formal analysis. **J.L. Santiago:** Writing – review & editing, Writing – original draft, Software, Resources, Methodology, Investigation, Formal analysis. **E. Rivas:** Software, Methodology, Investigation, Formal analysis. **J. Stocker:** Writing – review & editing, Writing – original draft, Software, Resources, Methodology, Investigation, Formal analysis. **R. Jackson:** Writing – review & editing, Software, Methodology, Formal analysis. **F. Russo:** Writing – review & editing, Writing – original draft, Software, Resources, Methodology, Investigation, Formal analysis. **M.G. Villani:** Software, Methodology, Investigation, Formal analysis. **G. Tinarelli:** Software, Methodology, Investigation, Formal analysis. **D. Barbero:** Software, Methodology, Investigation, Formal analysis. **R. San José:** Writing – review & editing, Writing – original draft, Software, Resources, Methodology, Investigation, Formal analysis. **J.L. Pérez-Camanyo:** Software, Methodology, Investigation, Formal analysis. **G. Sousa Santos:** Writing – review & editing, Writing – original draft, Software, Resources, Methodology, Investigation, Formal analysis. **J. Bartzis:** Writing – review & editing, Writing – original draft, Software, Resources, Methodology, Investigation, Formal analysis. **I. Sakellaris:** Software, Methodology, Investigation, Formal analysis. **Z. Horváth:** Writing – review & editing, Writing – original draft, Software, Resources, Methodology, Investigation, Formal analysis. **L. Környei:** Writing – review & editing, Writing – original draft, Software, Resources, Methodology, Investigation, Formal analysis. **B. Liszkai:** Software, Methodology, Investigation, Formal analysis. **Á. Kovács:** Software, Methodology, Investigation, Formal analysis. **X. Jurado:** Writing – review & editing, Writing – original draft, Software, Resources, Methodology, Investigation, Formal analysis. **N. Reiminger:** Writing – review & editing, Writing – original draft, Software, Resources, Methodology, Investigation, Formal analysis. **P. Thunis:** Writing – original draft, Supervision, Project administration, Investigation, Funding acquisition, Formal analysis. **C. Cuvelier:** Visualization, Software, Methodology, Investigation, Formal analysis.

Declaration of competing interest

The authors declare that they have no known competing financial interests or personal relationships that could have appeared to influence the work reported in this paper.

Data availability

Data will be made available on request.

Acknowledgements

Funded by the European Union. Part of this work has received funding from the European High Performance Computing Joint Undertaking (JU) and Poland, Germany, Spain, Hungary, France under grant agreement number: 101093457.

Disclaimer

Funded by the European Union. Views and opinions expressed are however those of the author(s) only and do not necessarily reflect those of the European Union or the European High Performance Computing Joint Undertaking (JU) and Poland, Germany, Spain, Hungary, France. Neither the European Union nor the granting authority can be held responsible for them.

Appendix A. Supplementary data

Supplementary data to this article can be found online at https://doi.org/10.1016/j.scitotenv.2024.171761.

References

Amorim, J.H., Rodrigues, V., Tavares, R., Valente, J., Borrego, C., 2013. CFD modelling of the aerodynamic effect of trees on urban air pollution dispersion. Sci. Total Environ. 461-462, 541–551.

Bady, M., 2014. Evaluation of Gaussian plume model against CFD simulations through the estimation of CO and NO concentrations in an urban area. Am. J. Environ. Sci. 13 (2) https://doi.org/10.3844/ajessp.2017.93.102, 93.102 2017.

Barbero, D., Tinarelli, G., Silibello, C., Nanni, A., Gariazzo, C., Stafoggia, M., Viegi, G., 2021. A microscale hybrid modelling system to assess the air quality over a large portion of a large European city. Atmos. Environ. 264, 118656.

Bartzis, J.G., Efthimiou, G.C., Andronopoulos, S., 2015. Modelling short term individual exposure from airborne hazardous releases in urban environments. J. Hazard. Mater. 300, 182–188.

Bartzis, J., Andronopoulos, S., Efthimiou, G., 2020a. Simplified approaches in quantifying exposure statistical behaviour due to airborne hazardous releases of short time duration. In: Proceedings of Abstracts 12th International Conference on Air Quality Science and Application, Thessaloniki, Greece.

Bartzis, J.G., Kalimeri, K.K., Sakellaris, I.A., 2020b. Environmental data treatment to support exposure studies: the statistical behavior for NO2, O3, PM10 and PM2.5 air concentrations in Europe. Environ. Res. 181, 108864.

Bartzis, J.G., Efthimiou, G.C., Andronopoulos, S., 2021. Modelling exposure from airborne hazardous short-duration releases in urban environments. Atmosphere 12 (2).

Bartzis, J.G., Sakellaris, I.A., Efthimiou, G., 2022. On exposure uncertainty quantification from accidental airborne point releases. J. Hazard. Mater. Adv. 6, 100080.

Belda, M., Resler, J., Geletic, J., Krc, P., Maronga, B., Sühring, M., Kurppa, M., Kanani-Sühring, F., Fuka, V., Eben, K., Benešová, N., Auvinen, M., 2021. Sensitivity analysis of the PALM model system 6.0 in the urban environment. Geosci. Model Dev. 14 (7), 4443–4464.

Biggart, M., Stocker, J., Doherty, R.M., Wild, O., Hollaway, M., Carruthers, D., Li, J., Zhang, Q., Wu, R., Kotthaus, S., Grimmond, S., Squires, F.A., Lee, J., Shi, Z., 2020. Street-scale air quality modelling for Beijing during a winter 2016 measurement campaign. Atmos. Chem. Phys. 20 (5), 2755–2780.

Borge, R., Santiago, J.L., de la Paz, D., Martín, F., Domingo, J., Valdés, C., Sánchez, B., Rivas, E., Rozas, M.T., Lázaro, S., Pérez, J., Fernández, A., 2018. Application of a short term air quality action plan in Madrid (Spain) under a high-pollution episode - part II: assessment from multi-scale modelling. Sci. Total Environ. 635, 1574–1584.

Carissimo, B., Trini Castelli, S., Tinarelli, G., 2021. JRII special sonic anemometer study: a first comparison of building wakes measurements with different levels of numerical modelling approaches. Atmos. Environ. 244, 117798.

Carruthers, D.J., Holroyd, R.J., Hunt, J.C.R., Weng, W.S., Robins, A.G., Apsley, D.D., Thompson, D.J., Smith, F.B., 1994. UK-ADMS: a new approach to modelling dispersion in the earth's atmospheric boundary layer. J. Wind Eng. Ind. Aerodyn. 52, 139–153.

De Craemer, S., Vercauteren, J., Fierens, F., Lefebvre, W., Meysman, F.J.R., 2020. Using large-scale no2 data from citizen science for air-quality compliance and policy support. Environ. Sci. Technol. 54 (18), 11070–11078.

EC, 2008. Directive 2008/50/EC of the European Parliament and of the Council of 21 may 2008 on ambient air quality and cleaner air for Europe (No. In: OJL, 152. European Parliament, Council of the European Union.

EEA, 2023. Europe's air quality status 2023. Briefing no. 05/2023. ISBN: ISBN: 978-92-9480-554-6 - ISSN: 2467-3196 - doi: 10.2800/59526, European Environment Agency. https://www.eea.europa.eu/publications/europes-air-quality-status-2023.

Haeger-Eugensson, M., et al., 2021. Air quality modeling in dense urban areas at ground level—CFD, OSM or Gauss? In: Mensink, C., Matthias, V. (Eds.), Air Pollution Modeling and its Application XXVII. ITM 2019. Springer Proceedings in Complexity. Springer, Berlin, Heidelberg. https://doi.org/10.1007/978-3-662-63760-9_37.

Hamer, P.D., Walker, S.-E., Sousa-Santos, G., Vogt, M., Vo-Thanh, D., Lopez-Aparicio, S., Schneider, P., Ramacher, M.O.P., Karl, M., 2020. The urban dispersion model EPISODE v10.0 –part 1: an Eulerian and sub-grid-scale air quality model and its application in Nordic winter conditions. Geosci. Model Dev. 13 (9), 4323–4353.

Hood, C., Stocker, Jenny, Seaton, Martin, Johnson, Kate, O'Neill, James, Thorne, Lewis, Carruthers, D., 2021. Comprehensive evaluation of an advanced street canyon air pollution model. J. Air Waste Manage. Assoc. 71 (2), 247–267.

Hooyberghs, H., De Craemer, S., Lefebvre, W., Vranckx, S., Maiheu, B., Trimpeneers, E., Vanpoucke, C., Janssen, S., Meysman, F.J.R., Fierens, F., 2022. Validation and optimization of the atmo-street air quality model chain by means of a large-scale citizen-science dataset. Atmos. Environ. 272, 118946.

Horváth, Z., Liszkai, B., Istenes, G., Zsebők, P., Szintai, B., Rácz, É.V.P., Környei, L., Harmati, I., 2016. Integrated urban air pollution dispersion modelling framework and application in air quality prediction of the city of Győr. In: Proceedings of the 17th International Conference on Harmonisation Within Atmospheric Dispersion Modelling for Regulatory Purposes.

Janssen, S., Dumont, G., Fierens, F., Mensink, C., 2008. Spatial interpolation of air pollution measurements using corine land cover data. Atmos. Environ. 42 (20), 4884–4903.

Jurado, X., Reiminger, N., Vazquez, J., Wemmert, C., 2021. On the minimal wind directions required to assess mean annual air pollution concentration based on CFD results. Sustain. Cities Soc. 71, 102920.

Jurado, X., Reiminger, N., Benmoussa, M., Vazquez, J., Wemmert, C., 2022. Deep learning methods evaluation to predict air quality based on computational fluid dynamics. Expert Syst. Appl. 203, 117294.

Jurado, X., Reiminger, N., Maurer, L., Vazquez, J., Wemmert, C., 2023. Assessment of a deep learning model for monitoring atmospheric pollution: case study in Antwerp, Belgium. Sustain. Cities Soc. 99, 104951.

Környei, L., Horváth, Z., Ruopp, A., Kovacs, A., Liszkai, B., 2021. Multi-scale modelling of urban air pollution with coupled weather forecast and traffic simulation on HPC architecture. In: Proceedings of the International Conference on High Performance Computing in Asia-Pacific Region Companion (HPC Asia 2021).

Maronga, B., Gross, G., Raasch, S., Banzhaf, S., Forkel, R., Heldens, W., Kanani-Sühring, F., Matzarakis, A., Mauder, M., Pavlik, D., Pfafferott, J., Schubert, S., Seckmeyer, G., Sieker, H., Winderlich, K., 2019. Development of a new urban climate model based on the model palm – project overview, planned work, and first achievements. Meteorol. Z. 28 (2), 105–119.

Martin, F., Fileni, L., Palomino, I., Vivanco, M.G., Garrido, J.L., 2014. Analysis of the spatial representativeness of rural background monitoring stations in Spain. Atmos. Pollut. Res. 5 (4), 779–788.

Oldrini, O., Armand, P., Duchenne, C., Olry, C., Moussafir, J., Tinarelli, G., 2017. Description and preliminary validation of the PMSS fast response parallel atmospheric flow and dispersion solver in complex built-up areas. Environ. Fluid Mech. 17, 997–1014.

Oliveira, K., Rodrigues, V., Slingerland, S., Vanherle, K., Soares, J., Rafael, S., Trozzi, C., Bouman, E.A., Ferreira, J., Kewo, A., Nielsen, P.S., Diafas, I., Monteiro, A., Miranda, A.I., Lopes, M., Hayes, E., 2022. Assessing the impacts of citizen-led policies on emissions, air quality and health. J. Environ. Manag. 302, 114047.

Owen, B., Edmunds, H.A., Carruthers, D.J., Singles, R.J., 2000. Prediction of total oxides of nitrogen and nitrogen dioxide concentrations in a large urban area using a new generation urban scale dispersion model with integral chemistry model. Atmos. Environ. 34 (3), 397–406.

Paden, I., García-Sánchez, C., Ledoux, H., 2022. Towards automatic reconstruction of 3D city models tailored for urban flow simulations. Front. Built Environ. 8.

Parra, M.A., Santiago, J.L., Martín, F., Martilli, A., Santamaría, J.M., 2010. A methodology to urban air quality assessment during large time periods of winter using computational fluid dynamic models. Atmos. Environ. 44 (17), 2089–2097.

Pullen, J., Boris, J.P., Young, T., Patnaik, G., Iselin, J., 2005. A comparison of contaminant plume statistics from a Gaussian puff and urban CFD model for two large cities. Atmos. Environ. 39 (6), 1049–1068. ISSN 1352-2310,. https://doi.org/10.1016/j.atmosenv.2004.10.043.

Rafael, S., Vicente, B., Rodrigues, V., Miranda, A.I., Borrego, C., Lopes, M., 2018. Impacts of green infrastructures on aerodynamic flow and air quality in Porto's urban area. Atmos. Environ. 190, 317–330.

Rafael, S., Rodrigues, V., Oliveira, K., Coelho, S., Lopes, M., 2021. How to compute long-term averages for air quality assessment at urban areas? Sci. Total Environ. 795, 148603.

Reiminger, N., Jurado, X., Vazquez, J., Wemmert, C., Blond, N., Wertel, Jonathan, Dufresne, Matthieu, 2020a. Methodologies to assess mean annual air pollution concentration combining numerical results and wind roses. Sustain. Cities Soc. 59, 102221.

Reiminger, N., Vazquez, J., Blond, N., Dufresne, M., Wertel, J., 2020b. CFD evaluation of mean pollutant concentration variations in step-down street canyons. J. Wind Eng. Ind. Aerodyn. 196, 104032.
Rivas, E., Santiago, J.L., Lechón, Y., Martín, F., Arino, A., Pons, J.J., Santamaría, J.M., 2019. CFD modelling of air quality in Pamplona City (Spain): assessment, stations spatial representativeness and health impacts valuation. Sci. Total Environ. 649, 1362–1380.
Rodrigues, V., Gama, C., Ascenso, A., Oliveira, K., Coelho, S., Monteiro, A., Hayes, E., Lopes, M., 2021. Assessing air pollution in European cities to support a citizen centered approach to air quality management. Sci. Total Environ. 799, 149311.
Russo, F., Villani, M.G., D'Elia, I., D'Isidoro, M., Liberto, C., Piersanti, A., Tinarelli, G., Valenti, G., Ciancarella, L., 2021. A study of traffic emissions based on floating car data for urban scale air quality applications. Atmosphere 12 (8).
Sakellaris, I.A., Bartzis, J.G., Neuhäuser, J., Friedrich, R., Gotti, A., Sarigiannis, D.A., 2022. A novel approach for air quality trend studies and its application to European urban environments: the ICARUS project. Atmos. Environ. 273, 118973.
San José, R., Perez-Camanyo, J.L., 2022. Modelling effects of type of trees on urban air pollution with a computational fluid dynamics model. Euro-Mediterr. J. Environ. Integr. 7, 381–389.
San José, R., Perez-Camanyo, J.L., 2023. High-resolution impacts of green areas on air quality in Madrid. Air Qual. Atmos. Health 16, 37–48.
Sanchez, B., Santiago, J.L., Martilli, A., Palacios, M., Kirchner, F., 2016. CFD modeling of reactive pollutant dispersion in simplified urban configurations with different chemical mechanisms. Atmos. Chem. Phys. 16 (18), 12143–12157.
San José, R., Perez-Camanyo, J.L., Gonzalez-Barras, R.M., 2021. The use of LES CFD urban models and mesoscale air quality models for urban air quality simulations. In: Studies in Systems. Decis. Control 7, 185–199.
Sanchez, B., Santiago, J.L., Martilli, A., Martin, F., Borge, R., Quaassdorff, C., de la Paz, D., 2017. Modelling NOx concentrations through CFD-RANS in an urban hot-spot using high resolution traffic emissions and meteorology from a mesoscale model. Atmos. Environ. 163, 155–165.
Santiago, J.L., Martin, F., 2015. Use of CFD modeling for estimating spatial representativeness of urban air pollution monitoring sites and suitability of their locations. In: Fisica de la Tierra, pp. 191–221.
Santiago, J.L., Martilli, A., Martin, F., 2007. CFD simulation of airflow over a regular array of cubes. Part I: three-dimensional simulation of the flow and validation with wind-tunnel measurements. Bound.-Layer Meteorol. 122, 609–634.
Santiago, J.L., Martín, F., Martilli, A., 2013. A computational fluid dynamic modelling approach to assess the representativeness of urban monitoring stations. Sci. Total Environ. 454-455, 61–72.
Santiago, J.L., Borge, R., Martin, F., de la Paz, D., Martilli, A., Lumbreras, J., Sanchez, B., 2017. Evaluation of a CFD-based approach to estimate pollutant distribution within a real urban canopy by means of passive samplers. Sci. Total Environ. 576, 46–58.
Santiago, J.L., Borge, R., Sanchez, B., Quaassdorff, C., de la Paz, D., Martilli, A., Rivas, E., Martín, F., 2021. Estimates of pedestrian exposure to atmospheric pollution using high-resolution modelling in a real traffic hot-spot. Sci. Total Environ. 755, 142475.
Santiago, J.L., Rivas, E., Sanchez, B., Buccolieri, R., Esposito, A., Martilli, A., Martín, F., 2022. Impact of different combinations of green infrastructure elements on traffic-related pollutant concentrations in urban areas. Atmosphere 13 (8), 1195.
Schatzmann, M., Leitl, B., 2011. Issues with validation of urban flow and dispersion CFD models. J. Wind Eng. Ind. Aerodyn. 99 (4), 169–186.
Sousa, J., Gorlé, C., 2019. Computational urban flow predictions with Bayesian inference: validation with field data. Build. Environ. 154, 13–22.
Sousa, J., García-Sánchez, C., Gorlé, C., 2018. Improving urban flow predictions through data assimilation. Build. Environ. 132, 282–290.
Trini, Castelli S., Armand, P., Tinarelli, G., Duchenne, C., Nibart, M., 2018. Validation of a Lagrangian particle dispersion model with wind tunnel and field experiments in urban environment. Atmos. Environ. 193, 273–289.
Tripathi, A., Souprayen, C., Stanley, A., Warrilow, N., 2018. Computational fluid dynamics or Gaussian – is there a right way to model gas dispersion?. In: Proc. of the 10th IMA International Conference on Modelling in Industrial Maintenance and Reliability, ISBN 978-0-905091-32-7.
Veratti, G., Fabbi, S., Bigi, A., Lupascu, A., Tinarelli, G., Teggi, S., Brusasca, G., Butler, T. M., Ghermandi, G., 2020. Towards the coupling of a chemical transport model with a micro-scale Lagrangian modelling system for evaluation of urban NOx levels in a European hotspot. Atmos. Environ. 223, 117285.
Viana, M., de Leeuw, F., Bartonova, A., Castell, N., Ozturk, E., González Ortiz, A., 2020. Air quality mitigation in European cities: status and challenges ahead. Environ. Int. 143, 105907.
Villani, M.G., Russo, F., Adani, M., Piersanti, A., Vitali, L., Tinarelli, G., Ciancarella, L., Zanini, G., Donateo, A., Rinaldi, M., Carbone, C., Decesari, S., Sänger, P., 2021. Evaluating the impact of a wall-type green infrastructure on PM10 and NOx concentrations in an urban street environment. Atmosphere 12 (7).
Vivanco, M.G., Palomino, I., Vautard, R., Bessagnet, B., Martín, F., Menut, L., Jiménez, S., 2009. Multi-year assessment of photochemical air quality simulation over Spain. Environ. Model Softw. 24 (1), 63–73.
Vivanco, M.G., Garrido, J.L., Martín, F., Theobald, M.R., Gil, V., Santiago, J.L., Lechón, Y., Gamarra, A.R., Sánchez, E., Alberto, A., Bailador, A., 2021. Assessment of the effects of the Spanish National Air Pollution Control Programme on air quality. Atmosphere 12 (2).
Vranckx, S., Vos, P., Maiheu, B., Janssen, S., 2015. Impact of trees on pollutant dispersion in street canyons: a numerical study of the annual average effects in Antwerp, Belgium. Sci. Total Environ. 532, 474–483.
Zhong, J., Hood, C., Johnson, K., Stocker, J., Handley, J., Wolstencroft, M., Mazzeo, A., Cai, X., Bloss, W.J., 2021. Using task farming to optimise a street-scale resolution air quality model of the west midlands (UK). Atmosphere 12 (8).